CrossMark

ORIGINAL ARTICLE

An upper Paleogene shallowing-upward sequence in the southern Sandino Forearc Basin (NW Costa Rica): response to tectonic uplift

Goran Andjić[1] · Claudia Baumgartner-Mora[1] · Peter O. Baumgartner[1]

Abstract The Sandino Forearc Basin of western Nicaragua and northwestern Costa Rica (Central America) provides a Campanian to Pliocene sedimentary record. The study of the onshore part of the basin in northwestern Costa Rica reveals for the first time the occurrence of upper Paleogene shallow-marine siliciclastic and carbonate sequences. These sequences have remained undescribed so far and are grouped herein into two new lithostratigraphic units—the upper Eocene Junquillal Formation (Fm.) and the upper Oligocene Juanilla Fm. The upper Eocene Junquillal Fm. is characterized by storm-related, arenitic to conglomeratic deposits comprised in metric, massive amalgamated beds. The shallow shelfal environment of deposition is attested by the presence of hummocky and swaley cross-stratifications. The lithologies of the Junquillal Fm. were previously considered to be part of the underlying, deep-water turbiditic deposits of the Eocene Descartes Fm. The deposition of the Junquillal Fm. is indicative of tectonic uplift that forced regression, which affected the southeastern part of the Sandino Forearc Basin during the late Eocene. The upper Oligocene Juanilla Fm. unconformably overlies the Junquillal Fm. and occurs as a 25-m-thick, 700-m-wide outcrop on Isla Juanilla. It is composed essentially of nodular, coral framestones exhibiting massive, closely packed corals in growth position that are associated with coralline red algae and Larger Benthic Foraminifera (LBF). A late Oligocene age of the reef is attested by LBF assemblages occurring in two different facies. The Juanilla Fm. coral reef is a unique exposure, characterized by extensive constructed coral framework, and which has no equivalent in the Oligocene geological record of Central America. The reef grew on a short-lived, siliciclastic-poor tectonic high, which developed in relation to a lower Oligocene, basin-scale folding event in the Sandino Forearc Basin.

Keywords Coral reef · Larger Benthic Foraminifera · Tectonic uplift · Eocene · Oligocene · Sandino Basin · N-Costa Rica

✉ Goran Andjić
   goran.andjic@unil.ch

   Claudia Baumgartner-Mora
   claudia.baumgartner@unil.ch

   Peter O. Baumgartner
   peter.baumgartner@unil.ch

[1] Institut des Sciences de la Terre, Université de Lausanne, Bâtiment Géopolis, Bureau 3623, 1015 Lausanne, Switzerland

Introduction

Forearc basins represent one of the several geotectonic features developed in arc-trench systems of active margins (Dickinson and Seely 1979; Dickinson 1995). Forearc sedimentary sequences record the tectonic and volcanic activity of convergent margins and often remain the only source of information of its past evolution, especially if neotectonics and recent volcanism have obliterated part of the geological record. More specifically, the short-lived occurrence of shallow-marine carbonate and siliciclastic facies in predominantly deep-water forearc basins provides a record of tectonic uplift that interfered with eustatic sea-level changes, paleoclimate, and other paleoenvironmental conditions (Dorobek 2008). Ephemeral carbonate buildups can grow in siliciclastic–volcaniclastic settings if they are temporarily isolated from a direct input of detrital sediments (Braga and Martin 1988; Wilson and Lokier 2002; Wilson 2005; Bosence 2005; Dorobek 2008). The isolation

🖄 Springer

from a siliciclastic supply in a forearc context is achieved by the development of tectonically induced structural highs or sheltering from clastics in areas with reliefs such as shelf margins, abandoned lowstand delta margins, and lobes (Bosence 2005; Wilson and Hall 2010; Saller et al. 2011).

The Sandino Forearc Basin (SFB) corresponds to one of the many Upper Cretaceous–Tertiary forearc basins formed along the western margin of the Caribbean Plate (Dengo 1985; Alvarado et al. 2007). The SFB stratigraphy has been studied in northwestern Costa Rica and western Nicaragua for more than a century in the framework of several reference studies (Hayes 1899; Vaughan 1918; Dorr 1933; Harrison 1953; Hoffstetter et al. 1956; Zoppis Bracci and Del Giudice 1958; Dengo 1962; McBirney and Williams 1965; Kuang 1971; Schmidt-Effing 1974; Weyl 1980; Baumgartner et al. 1984; Astorga 1987, 1988; Kolb and Schmidt 1991; Winsemann 1992; Weinberg 1992; Krawinkel and Kolb 1994; Elming et al. 1998; Ranero et al. 2000; Walther et al. 2000; McIntosh et al. 2007; Struss et al. 2007, 2008;

Funk et al. 2009; Fig. 1). There are also numerous, informal studies and reports done for the petroleum industry (Petronic) and several Nicaraguan government institutes (INMINE, INE, SGAB, SAREC, INETER), which have never been published and remain mostly inaccessible (for example: Auer 1942; Wilson 1942; Williams 1972; Parsons Corporation Report 1972; Barboza et al. 1993; RECOPE-INE 1993). The present study focuses on the description, interpretation, and definition of two new, shelfal lithostratigraphic units, the upper Eocene Junquillal Fm. and the upper Oligocene Juanilla Fm., which crop out in the northern Costa Rican part of the SFB (Fig. 2). The existence of these new units represents a striking feature of the studied segment of the SFB. Previous studies of this area recognized only deep-water, turbiditic lithologies in the Tertiary record. The facies study of the Eocene–Oligocene stratigraphic succession reveals important paleoenvironmental and relative sea-level changes that shed light on the sedimentary and tectonic evolution of the SFB. The present
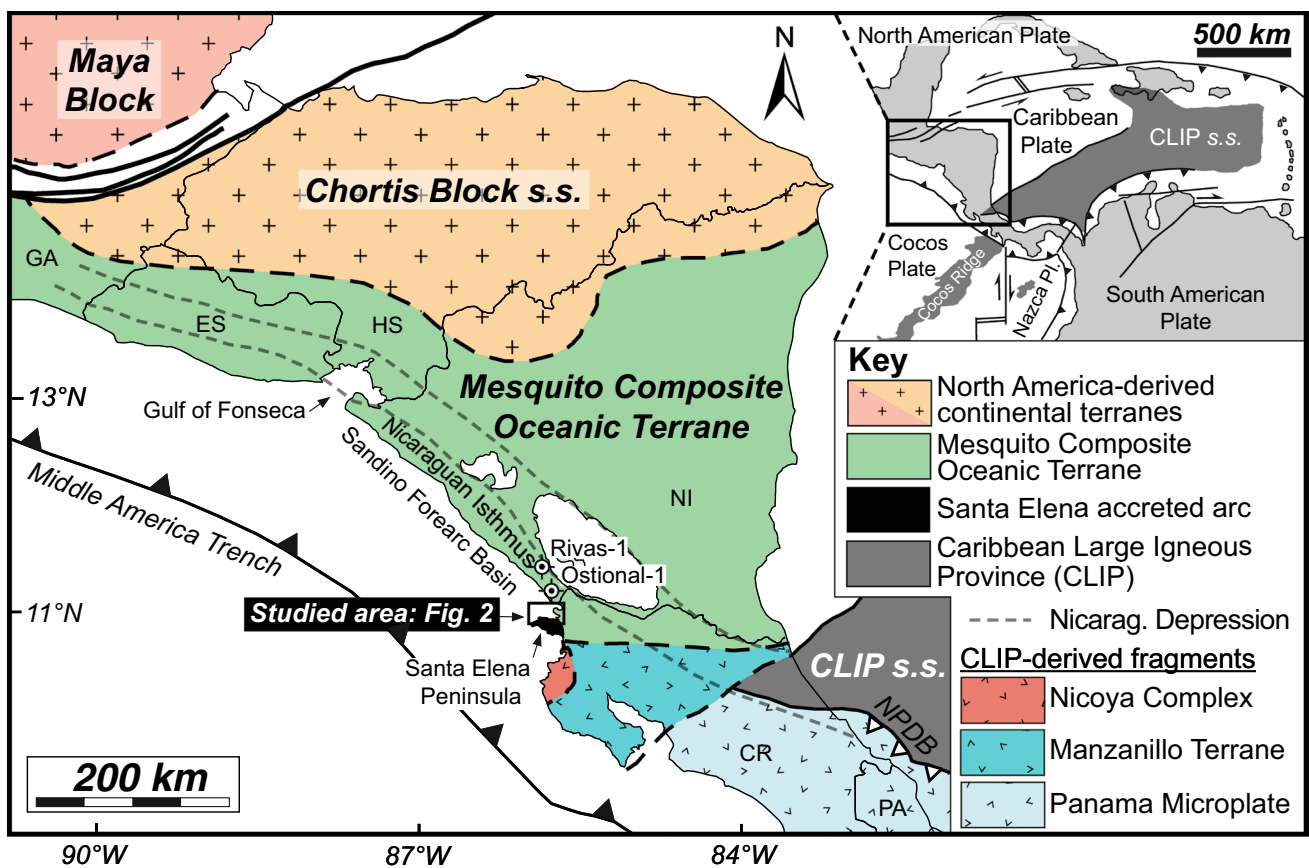

Fig. 1 Terrane map displaying the major structural features of the Central America arc-trench system, with the general tectonic plate setting of the Caribbean Plate in inset (*upper right*; modified after Baumgartner et al. 2008; Bandini et al. 2008; Flores 2009; Funk et al. 2009; Buchs et al. 2010). The studied area (*black rectangle*) is situated at the southeastern end of the Sandino Forearc Basin, in the Santa Elena Peninsula-Punta Descartes area (Costa Rica northwesternmost corner). The Rivas-1 and Ostional-1 boreholes are indicated. *NPDB* North Panama Deformed Belt, *CLIP* Caribbean Large Igneous Province, *GA* Guatemala, *ES* El Salvador, *HS* Honduras, *NI* Nicaragua, *CR* Costa Rica, *PA* Panama, *Nicarag. Depression* Nicaraguan Depression

study is part of a basin-scale investigation of the SFB and represents the first paper of a series that will adopt a similar approach for outcrops located in the Nicaraguan part of the basin.

Geological setting

The Sandino Forearc Basin (SFB) corresponds to a latest Cretaceous–Neogene forearc basin. The SFB presents both offshore and onshore parts that extend over a distance of 300 km from the Santa Elena Peninsula (NW Costa Rica) to the Gulf of Fonseca, which is situated at the intersection of the Nicaragua, Honduras and El Salvador borders (Ranero et al. 2000; Funk et al. 2009; Fig. 1). The offshore part of the SFB lies between the Nicaraguan Pacific coast and the Middle America Trench off Nicaragua (Ranero et al. 2000, 2007; Fig. 1). The depocenter of the basin is located in the vicinity of the coastline and is filled with ~10 km of forearc sequences that progressively thin towards an outer high (Ranero et al. 2000, 2007). The onshore geology of the SFB crops out in a 160-km-long/30-km-wide, slightly folded belt, exposed along the Nicaraguan Isthmus (Hodgson 1998; Darce and Duarte 2002; Figs. 1, 2). This 300-km-long isthmus is bordered to the east by normal and strike-slip faults that mark the limit with the Nicaraguan Depression (Fig. 1).

Classically, the Chortis Block *s.l.* was considered as the basement of the SFB (Dengo 1985). More recently, it became evident from few outcrops, geophysics and volcanic geochemistry that most of Nicaragua is underlain by the Mesquito Composite Oceanic Terrane (MCOT), which represents Franciscan-type, accreted terranes with oceanic remnants in a serpentinitic matrix (Rogers et al. 2007; Baumgartner et al. 2008; Fig. 1). To the south, the MCOT is bounded by a complex puzzle of Mesozoic plateau-like oceanic terranes that crop out in northwestern Costa Rica (Baumgartner and Denyer 2006; Baumgartner et al. 2008; Bandini et al. 2008; Buchs et al. 2010; Fig. 1).

Escuder-Viruete and Baumgartner (2014) proposed that the Santa Elena tectonic pile corresponds to an intraoceanic arc that became accreted to the MCOT during Late Cretaceous time. Escuder-Viruete et al. (2015) revalidate the term "ophiolite" for the Santa Elena ultramafic nappe, based on the observation of the paleo-Moho and overlying layered and massive gabbros (Isla Negritos gabbros; Fig. 2) along the top of the main body.

The SFB deposits overlap this area of terrane collage rendering its internal limits unobservable. In the southeasternmost segment of the SFB, the forearc sequences deposited over the essentially ultramafic, tectonic pile exposed in the Santa Elena Peninsula (Baumgartner et al. 1984; Escuder-Viruete and Baumgartner 2014). In the Nicaraguan part of the SFB, the underlying basement is poorly known. Supposedly it is part of the MCOT. In one of two onshore drill holes (Rivas-1; Fig. 1) the oldest lithologies of the SFB consist of volcaniclastic to tuffaceous deep-water sediments underlain by a basaltic basement of unknown origin (Ranero et al. 2000; Fig. 2).

During Campanian to Oligocene, predominantly deepwater pelagic, hemipelagic and turbiditic sequences are successively replaced by platform siliciclastics and carbonates at different steps of the basin evolution (Zoppis Bracci and Del Giudice 1958; Elming et al. 1998). The initial stage of basin development only crops out in the Santa Elena Peninsula (NW Costa Rica; Fig. 2), where the basement of the southeastern part of the basin is overlain by a veneer of shallow-water limestones followed by deep-water sedimentary sequences deposited in Latest Cretaceous–Eocene times (Zoppis Bracci and Del Giudice 1958; Dengo 1962; Baumgartner et al. 1984; Astorga 1987, 1988; Winsemann 1992). The Santa Elena Peninsula consists mainly of an ultramafic nappe made of serpentinized peridotites cut by mafic dykes and overlain by massive and sheeted gabbros, interpreted as a piece of a supra-subduction zone mantle and crust of unknown age (Santa Elena ultramafic nappe; Harisson 1953; Azéma and Tournon 1980, 1982; Tournon 1994; Hauff et al. 2000; Baumgartner and Denyer 2006; Gazel et al. 2006; Zaccarini et al. 2011; Escuder-Viruete and Baumgartner 2014; Santa Elena ophiolite, Escuder-Viruete et al. 2015). The Santa Elena ultramafic nappe thrusted onto a relative autochthonous accretionary complex, known as the Santa Rosa Accretionary Complex (Baumgartner and Denyer 2006; Escuder-Viruete and Baumgartner 2014), built up by the stacking of several tectonic units (Tournon 1984; Baumgartner and Denyer 2006). A gap in the dated sedimentary record exists between the youngest rocks observed in the nappe edifice (Albian; Bandini et al. 2011) and the oldest rocks (upper Campanian) of the sedimentary cover overlapping the ultramafic nappe. Intraoceanic accretion must have occurred since the Albian, while a hypothetical arc–arc collision and final overthrust of the Santa Elena ultramafic nappe must have occurred shortly prior to the late Campanian (Escuder-Viruete and Baumgartner 2014). Tectonic uplift resulted in local emersion and the deposition of the shallow-water El Viejo Formation, characterized by upper Campanian rudist biostromes (Schmidt-Effing 1974, 1980; Seyfried and Sprechmann 1985) and associated periplatform to slope deposits (e.g., Bahia Santa Elena outcrops; Di Marco et al. 1995; Baumgartner-Mora and Denyer 2002; Figs. 2, 3). Reworked ultramafic and mafic clasts of the underlying nappe are observed in all the lithologies of the El Viejo Fm. and suggest an original sedimentary contact with the ultramafic/mafic basement, which we have mapped in 2015. This observation is in contradiction with the existence of a
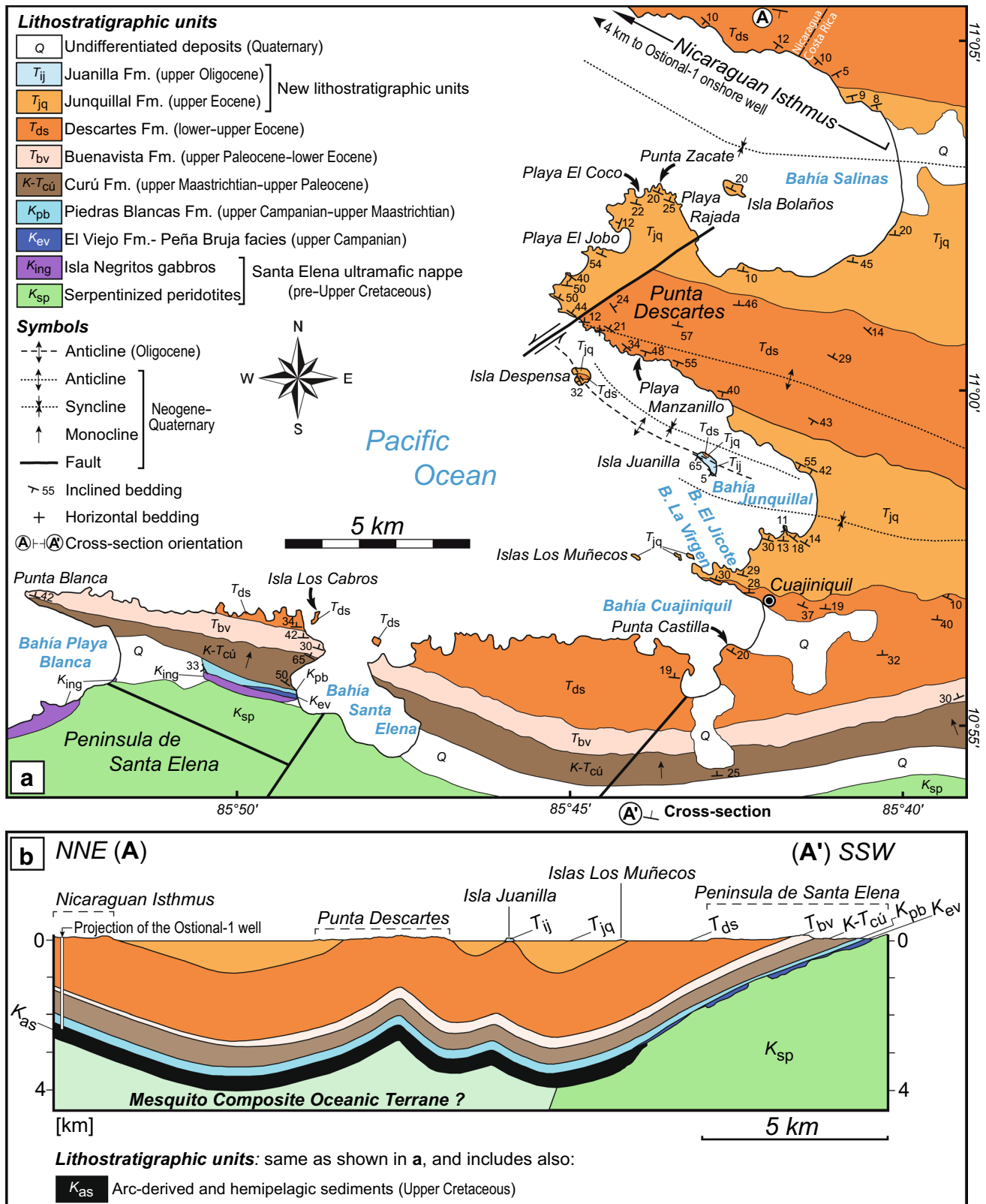
a

Lithostratigraphic units

- Q — Undifferentiated deposits (Quaternary)
- T_{ij} — Juanilla Fm. (upper Oligocene) ⎤ New lithostratigraphic units
- T_{jq} — Junquillal Fm. (upper Eocene) ⎦
- T_{ds} — Descartes Fm. (lower-upper Eocene)
- T_{bv} — Buenavista Fm. (upper Paleocene-lower Eocene)
- K-$T_{cú}$ — Curú Fm. (upper Maastrichtian-upper Paleocene)
- K_{pb} — Piedras Blancas Fm. (upper Campanian-upper Maastrichtian)
- K_{ev} — El Viejo Fm.- Peña Bruja facies (upper Campanian)
- K_{ing} — Isla Negritos gabbros ⎤ Santa Elena ultramafic nappe
- K_{sp} — Serpentinized peridotites ⎦ (pre-Upper Cretaceous)

Symbols

- Anticline (Oligocene)
- Anticline ⎤
- Syncline ⎥ Neogene-Quaternary
- Monocline ⎥
- Fault ⎦
- ⊢55 Inclined bedding
- + Horizontal bedding
- Ⓐ⊢Ⓐ' Cross-section orientation

b NNE (**A**)   (**A'**) SSW

Lithostratigraphic units: same as shown in **a**, and includes also:

- K_{as} — Arc-derived and hemipelagic sediments (Upper Cretaceous)

◄**Fig. 2 a** New geological map of the Santa Elena-Punta Descartes area (Sandino Forearc Basin; modified after Dengo 1962; Baumgartner et al. 1984; Astorga 1987; Denyer and Alvarado 2007; Escuder-Viruete et al. 2015). The mapped area encompasses the 1:50,000 topographic map sheets 3048 I (Murciélago), 3048 IV (Santa Elena) and 3049 II (Bahia Salinas) of the National Geographic Institute of Costa Rica. The detailed description of the mapped lithostratigraphic units is presented in the Fig. 3. We introduce two new lithostratigraphic units, the Junquillal Fm. and the Juanilla Fm., which have been previously mapped as Descartes Fm. The localities mentioned in the text and the position of the cross section (A–A', **b** of the same figure) are indicated. **b** NNE–SSW-oriented cross section (A–A', no vertical exaggeration) set perpendicular to the main tectonic structures of the Santa Elena-Punta Descartes area. The cross section displays one informal unit (Kas), which is not exposed in the mapped area shown in **a**. This unit corresponds to Upper Cretaceous arc-derived, tuffaceous sediments, which underlie the upper Campanian–upper Maastrichtian Piedras Blancas Fm. and are only known from the Ostional-1 and Rivas-1 boreholes drilled in Nicaragua (see Fig. 1 for borehole locations, Ranero et al. 2000). These Upper Cretaceous arc-derived sediments overlie a basaltic terrane possibly associated to the Mesquito Composite Oceanic Terrane (Baumgartner et al. 2008) and which was recovered from the Rivas-1 borehole (Ranero et al. 2000). Such sediments are not known to overly the Santa Elena tectonic pile (in the field), possibly due to the Campanian tectonic event (see text). We induce a subcrop contact between the basaltic terrane (Mesquito Composite Oceanic Terrane) and the Santa Elena ultramafic nappe. This terrane boundary is tentatively indicated on the cross section beneath the Bahia Cuajiniquil, given the absence of data on this subject

major fault, prolonging the trace of the Hess Escarpment, between the Santa Elena serpentinites and the overlying sediments, as drawn for instance by Meschede and Frisch (1998, "Santa Elena Fault") and Giunta et al. (2006). The El Viejo Fm. represents the oldest formation in this part of the SFB (Figs. 2, 3).

The Campanian shallow-water and periplatform deposits are overlain by a pluri-kilometric forearc sequence exposed in large-scale, open folds with WNW–ESE-oriented axes exposed along the northern coast of the Santa Elena Peninsula and in Punta Descartes (Zoppis Bracci and Del Giudice 1958; Dengo 1962; Baumgartner et al. 1984; Astorga 1987, 1988; Winsemann 1992; Denyer and Alvarado 2007; Fig. 2). Similar deposits are known from the Nicoya Peninsula and the Nicoya Gulf (Dengo 1962; Schmidt-Effing 1979; Lundberg 1982; Rivier 1983; Astorga 1987, 1988; Flores et al. 2003a, b). The base of the deep-water sequence consists of hemipelagic, globotruncanid-rich limestones of the upper Campanian–upper Maastrichtian Piedras Blancas Fm. (Baumgartner et al. 1984; Astorga 1987, 1988; Di Marco et al. 1995; Figs. 2, 3). The upper Maastrichtian–upper Paleocene Curú Fm. (=Rivas Fm. in Nicaragua) conformably overlies the Piedras Blancas Fm. and marks the beginning of detrital forearc sedimentation in the area, with distal turbidites of mafic composition (Baumgartner et al. 1984; Astorga 1987, 1988). The overlying upper Paleocene–lower Eocene siliceous pelagic limestones of the Buenavista Fm. represent a break in the

turbiditic sedimentation (Baumgartner et al. 1984). This 300-m-thick formation is exposed on the northern shore of the Santa Elena Peninsula. The Eocene Descartes Fm. indicates the transition to a more evolved volcanic arc activity of its source, underlined by an acidic composition of the forearc turbidites (Astorga 1987, 1988).

Due to kilometric, open folding, the Descartes Fm. (=Brito Fm. in Nicaragua) covers the whole area between the northern coast of the Santa Elena Peninsula and the southeastern coast of Nicaragua, with several repetitions. The northern shore of the Santa Elena Peninsula and the southern coast of the Punta Descartes are composed of the most ancient and most distal sequences of the Descartes Fm. and correspond to distal turbidites (Baumgartner et al. 1984; Astorga 1987, 1988; Figs. 2, 3). On the other hand, the western-northwestern Punta Descartes and the area south of Bahia Junquillal show more recent and more proximal deposits (Dengo 1962; Baumgartner et al. 1984; Astorga 1987). In this paper, these deposits are defined as a new, upper Eocene formation, the Junquillal Fm. This formation corresponds to shelfal, storm-influenced detrital lithologies that were previously considered as deep-water, turbiditic deposits attributed to the Eocene Descartes Fm. The overlying Isla Juanilla Fm. forms an island (~0.2 km²), which represents the youngest deposits preserved in a synform cropping out in Bahia Junquillal (Fig. 2). The Juanilla Fm. represents a striking feature in comparison to the surrounding geological setting, as it is the only Tertiary shallow-water limestone outcrop in the northwesternmost corner of Costa Rica. Furthermore, the geology of this small island has remained until now undescribed. Field observations indicate that it consists mainly of a reef buildup of corals and red algae with local occurrences of Larger Benthic Foraminifera-rich outcrops.

Lithostratigraphy

Here, we reexamine the outcrops of the deep-water Descartes Fm. of the studied area, to clarify its differences, as compared to the newly established, shelfal Junquillal Fm. Additionally, we present the facies description and interpretation of the new Junquillal and Juanilla fms. (Figs. 3, 4, 5, 6, 7, 8). We dated the discussed lithostratigraphic units with Larger Benthic Foraminifera (LBF) recovered from several outcrops (Figs. 9, 10, 11). The samples that yielded valuable biostratigraphic data are mentioned within brackets in the text and in the figures (Figs. 3, 4, 7). The location and the extension of the described lithostratigraphic units are shown in Fig. 2. Their significance for the tectonic interpretation will be treated in the discussion (see below). The stratigraphic terminology used in the following paragraphs is based on Murphy and Salvador (1999).
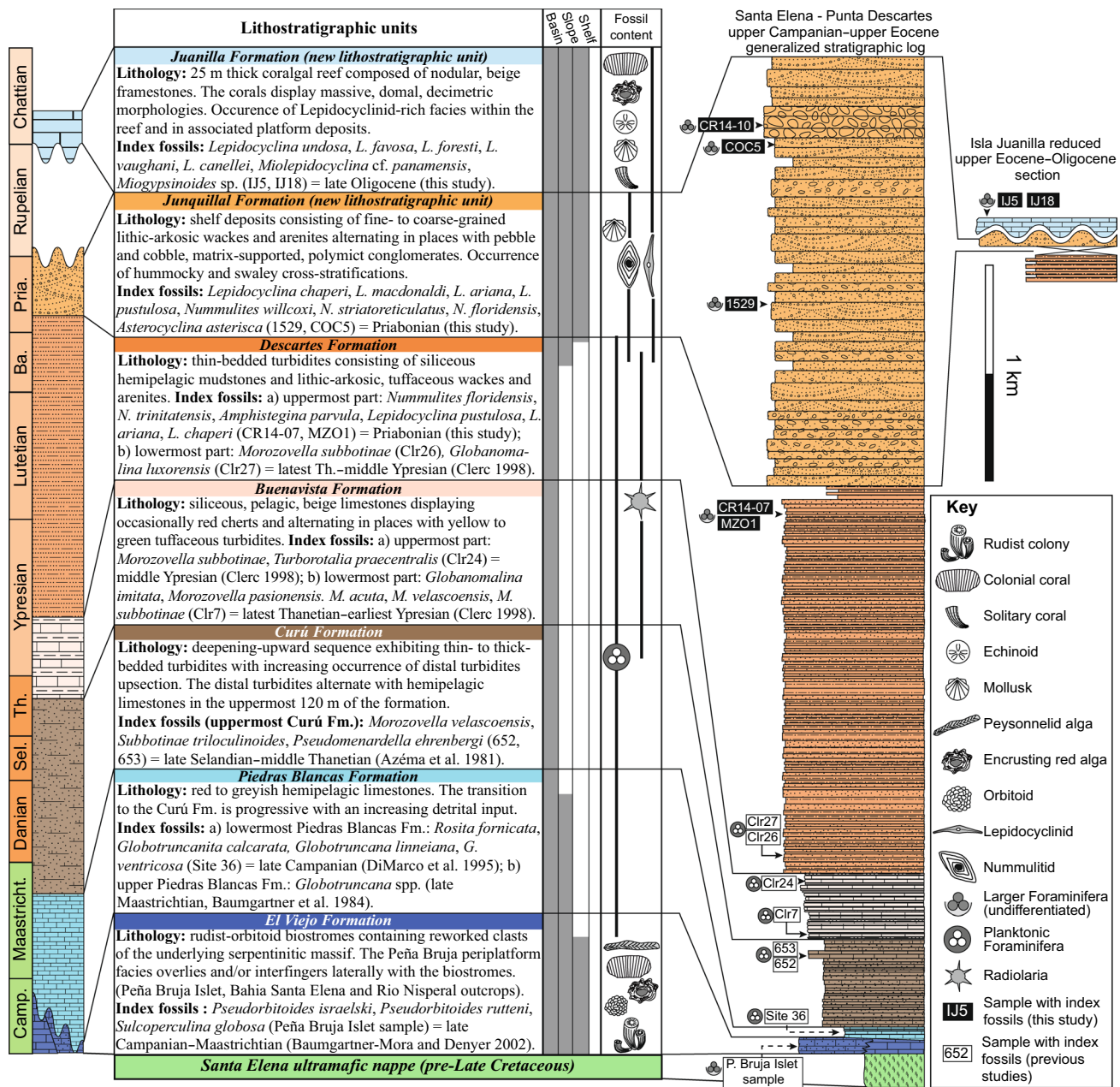
Lithostratigraphic units | Slope Basin / Shelf | Fossil content | Santa Elena - Punta Descartes upper Campanian–upper Eocene generalized stratigraphic log

Juanilla Formation (new lithostratigraphic unit)
Lithology: 25 m thick coralgal reef composed of nodular, beige framestones. The corals display massive, domal, decimetric morphologies. Occurence of Lepidocyclinid-rich facies within the reef and in associated platform deposits.
Index fossils: *Lepidocyclina undosa, L. favosa, L. foresti, L. vaughani, L. canellei, Miolepidocyclina* cf. *panamensis, Miogypsinoides* sp. (IJ5, IJ18) = late Oligocene (this study).

Junquillal Formation (new lithostratigraphic unit)
Lithology: shelf deposits consisting of fine- to coarse-grained lithic-arkosic wackes and arenites alternating in places with pebble and cobble, matrix-supported, polymict conglomerates. Occurrence of hummocky and swaley cross-stratifications.
Index fossils: *Lepidocyclina chaperi, L. macdonaldi, L. ariana, L. pustulosa, Nummulites willcoxi, N. striatoreticulatus, N. floridensis, Asterocyclina asterisca* (1529, COC5) = Priabonian (this study).

Descartes Formation
Lithology: thin-bedded turbidites consisting of siliceous hemipelagic mudstones and lithic-arkosic, tuffaceous wackes and arenites. **Index fossils:** a) uppermost part: *Nummulites floridensis, N. trinitatensis, Amphistegina parvula, Lepidocyclina pustulosa, L. ariana, L. chaperi* (CR14-07, MZO1) = Priabonian (this study); b) lowermost part: *Morozovella subbotinae* (Clr26), *Globanomalina luxorensis* (Clr27) = latest Th.–middle Ypresian (Clerc 1998).

Buenavista Formation
Lithology: siliceous, pelagic, beige limestones displaying occasionally red cherts and alternating in places with yellow to green tuffaceous turbidites. **Index fossils:** a) uppermost part: *Morozovella subbotinae, Turborotalia praecentralis* (Clr24) = middle Ypresian (Clerc 1998); b) lowermost part: *Globanomalina imitata, Morozovella pasionensis. M. acuta, M. velascoensis, M. subbotinae* (Clr7) = latest Thanetian–earliest Ypresian (Clerc 1998).

Curú Formation
Lithology: deepening-upward sequence exhibiting thin- to thick-bedded turbidites with increasing occurrence of distal turbidites upsection. The distal turbidites alternate with hemipelagic limestones in the uppermost 120 m of the formation.
Index fossils (uppermost Curú Fm.): *Morozovella velascoensis, Subbotinae triloculinoides, Pseudomenardella ehrenbergi* (652, 653) = late Selandian–middle Thanetian (Azéma et al. 1981).

Piedras Blancas Formation
Lithology: red to greyish hemipelagic limestones. The transition to the Curú Fm. is progressive with an increasing detrital input.
Index fossils: a) lowermost Piedras Blancas Fm.: *Rosita fornicata, Globotruncanita calcarata, Globotruncana linneiana, G. ventricosa* (Site 36) = late Campanian (DiMarco et al. 1995); b) upper Piedras Blancas Fm.: *Globotruncana* spp. (late Maastrichtian, Baumgartner et al. 1984).

El Viejo Formation
Lithology: rudist-orbitoid biostromes containing reworked clasts of the underlying serpentinitic massif. The Peña Bruja periplatform facies overlies and/or interfingers laterally with the biostromes. (Peña Bruja Islet, Bahia Santa Elena and Rio Nisperal outcrops).
Index fossils : *Pseudorbitoides israelski, Pseudorbitoites rutteni, Sulcoperculina globosa* (Peña Bruja Islet sample) = late Campanian–Maastrichtian (Baumgartner-Mora and Denyer 2002).

Santa Elena ultramafic nappe (pre-Late Cretaceous)

Isla Juanilla reduced upper Eocene–Oligocene section

Samples: CR14-10, COC5, 1529, CR14-07, MZO1, Clr27, Clr26, Clr24, Clr7, 653, 652, Site 36, P. Bruja Islet sample, IJ5, IJ18

1 km

Key
- Rudist colony
- Colonial coral
- Solitary coral
- Echinoid
- Mollusk
- Peysonnelid alga
- Encrusting red alga
- Orbitoid
- Lepidocyclinid
- Nummulitid
- Larger Foraminifera (undifferentiated)
- Planktonic Foraminifera
- Radiolaria
- IJ5 Sample with index fossils (this study)
- 652 Sample with index fossils (previous studies)

Chronostratigraphic column (left): Chattian, Rupelian, Pria., Ba., Lutetian, Ypresian, Th., Sel., Danian, Maastricht., Camp.

Fig. 3 General stratigraphy of the Sandino Forearc Basin units exposed in the northwesternmost corner of Costa Rica. The figure is divided into three distinct parts, from *left* to *right*: a chronostratigraphic column of the lithostratigraphic units (*left*), a three-column chart presenting the general description of the lithostratigraphic units (*middle*), and two stratigraphic logs of the studied area (*right*). The three parts are correlated with *continuous lines* representing the boundaries of the lithostratigraphic units. The three-column chart (*middle*) displays the characteristics of each lithostratigraphic unit. This include short lithological descriptions (=legend for the lithologies depicted in the *left* and *right* columns), lists of index fossils with corresponding authors and sample names, and indications on depositional environments and fossil contents. The fossil contents are not exhaustive and only the most common fossils are mentioned. The lists of index fossils (planktonic and Larger Benthic Foraminifera) are used to constrain the chronostratigraphic column (*left*) and originate from the present study (sample names with *black rectangles*) and from previous studies (sample names with *white rectangles*). The general stratigraphic logs (*right*) exhibit the thickness of each lithostratigraphic unit and the stratigraphic position of the samples containing index fossils

Descartes Formation: a formal definition

The Descartes Fm. corresponds to a commonly used informal unit name, introduced by Astorga (1987) in an unpublished work. A formal definition and a revision of this unit is necessary, since: (1) Astorga (1987) represents
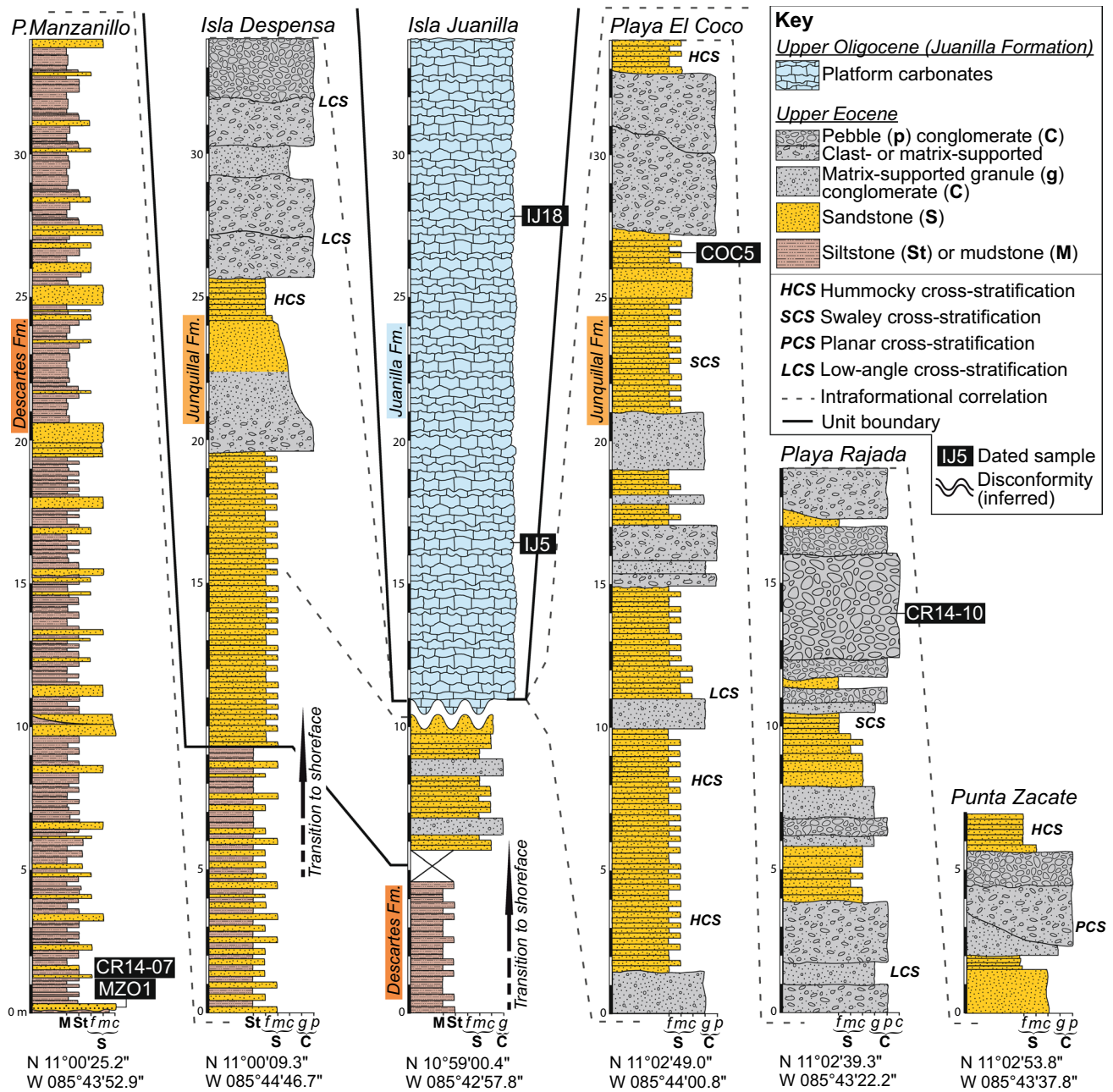
Fig. 4 Stratigraphic logs of the Punta Descartes-Bahia Junquillal area evidencing a transition from deep-water, turbiditic facies (Descartes Fm.) to siliciclastic (Junquillal Fm.) and carbonate (Juanilla Fm.) shallow shelf facies. The limits between the three lithostratigraphic units are depicted with *continuous lines*, whereas the *dashed lines* highlight the correlation within the units. The Playa Manzanillo section represents the lectostratotype of the Descartes Fm. (see text). For the newly established Junquillal Fm., the Playa Despensa section corresponds to the holostratotype (see text), whereas the Playa El Coco, the Playa Rajada and the Punta Zacate sections represent parastratotypes (see text). The samples that yielded biostratigraphic data are indicated within *black rectangles*. The GPS coordinates indicate the precise location of each section. The localities where the six sections were studied are shown on the geological map in Fig. 2. *P. Manzanillo* Playa Manzanillo

a work that was not published in a recognized scientific medium (see Murphy and Salvador 1999); (2) the lithologies of the upper part of the Descartes Fm. (sensu Astorga 1987) are excluded from the latter and grouped in a new, distinct unit herein defined as the Junquillal Fm. (see

below; Figs. 2, 3, 4). The siliceous pelagic limestones cropping out on the northern shore of the Santa Elena Peninsula (Fig. 2) were also included with the lower Descartes Fm. (Astorga 1987). Here, we consider these as a separate formation, the Buenavista Fm., as it was defined by
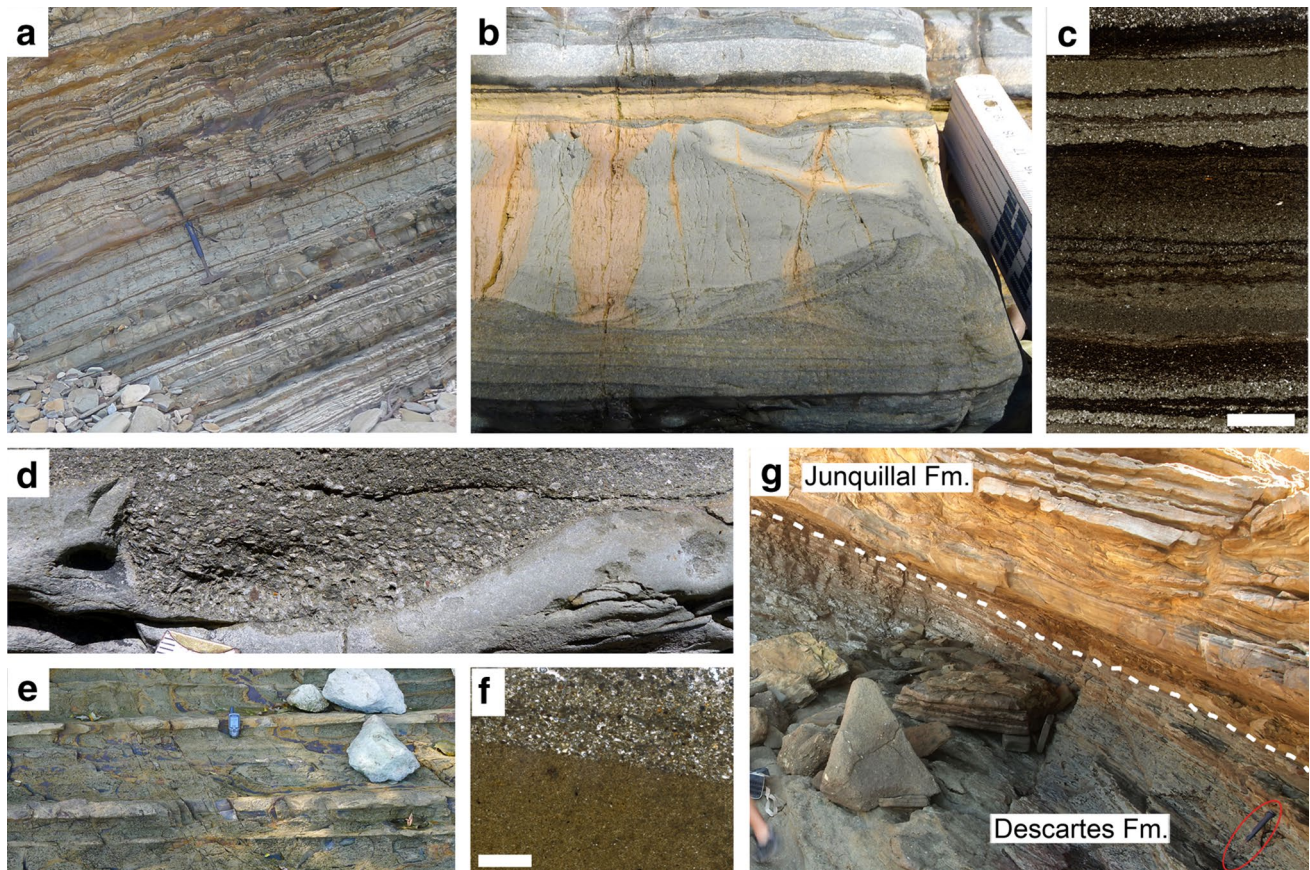
Fig. 5 Field photographs of the Eocene Descartes Fm. See Fig. 2 for locations. **a** Thin-bedded turbidites presenting centimetric alternations of silty/hemipelagic (*bright color*) and sandy (*dark color*) beds (Playa Manzanillo, N 11°00′25.2″/W 085°43′52.9″). *Hammer* length 31 cm. **b** Close-up view of a decimetric bed consisting of several turbiditic events (Punta Castilla, N 11°56′11.1″/W 085°42′33.8″). Note the *double meter stick* for scale. **c** Thin-section photomicrograph of mm- to cm-scale turbidites, which grade from very fine sand to radiolarian-bearing mud. *Scale bar* 5 mm. Same locality as in **b**. **d** Erosive contact between a LBF-rich, graded arenitic turbidite and the underlying mudstone (Playa Manzanillo). Note the *double meter stick* for scale. **e** Heterolithic facies (F1 in Fig. 7) consisting of centimetric to decimetric silty mudstones and centimetric, arkosic wackes (Isla Juanilla, N 10°58′58.3″/W 085°42′53.8″). *GPS device* length 14 cm. **f** Thin-section photomicrograph of the facies shown in **e**. *Scale bar* 1 mm. **g** Conformable contact between the silty-sandy lithologies of the uppermost Descartes Fm. and the sandy lithologies of the lowermost Junquillal Fm. (Isla Despensa, N 11°00′07.6″/W 085°44′48.8″). *Hammer* length 31 cm

Baumgartner et al. (1984; Figs. 2, 3). The general definition of the Descartes Fm. remains unchanged. The aspects of the Descartes Fm. examined hereafter are essentially based on our observations in the Santa Elena Peninsula-Punta Descartes area that represents the type area of the Descartes Fm. (Fig. 2).

Stratotype and reference sections

The type locality was informally defined in the Punta Descartes Peninsula by Astorga (1987, unpublished work). However, he omitted to establish and localize a holostratotype. The well-preserved exposures located at the Playa Manzanillo (N 11°00′28.5″/W 085°43′57.2″; Figs. 2, 4, 5a) and in the vicinity (southern Punta Descartes) constitute a continuous 160-m-thick section that is regarded here as a lectostratotype section. The coastal outcrops exposed along the western Punta Descartes are excluded from the Descartes Fm. and included into the Junquillal Fm.

Numerous characteristic, well-preserved coastal exposures of the Descartes Fm. can be observed on the northern shore of the Santa Elena Peninsula. The Punta Castilla section (N 10°56′11.1″/W 085°42′33.8″; Fig. 2) represents the best preserved and the most easily accessible outcrop of this area and is here considered as a hypostratotype section.

Formation boundaries

The lower boundary is defined at the beach located 240 m southwest of the Isla Los Cabros (N 10°56′27.0″/W 085°48′57.4″; Fig. 2) by an abrupt change from the beige, siliceous pelagic limestones of the Buenavista Fm. to the

conformably overlying, brown and green, fine-grained turbidites of the Descartes Fm.

The upper boundary is defined on the Isla Despensa (N 11°00′07.6″/W 085°44′48.8″; Figs. 2, 4, 5g) by an abrupt change from a heterolithic facies of the Descartes Fm., consisting of silty-sandy alternations, to the conformably overlying, amalgamated medium-grained sandstones of the Junquillal Fm. The boundary between the two formations is also evident from the outcrop morphology. The silty lithologies of the uppermost Descartes Fm. were strongly scoured by wave action in comparison to the competent, sandy lithologies of the overlying Junquillal Fm. The upper boundary of the formation is also observed on the northern shore of the Bahia Cuajiniquil (N 10°57′11.1″/W 085°42′55.8″; Fig. 2) with the transition from thin- to thick-bedded turbidites of the Descartes Fm. to the thick- to massive-bedded, amalgamated arenites of the Junquillal Fm.

Derivation of the name and synonymy

The formation is named after the Punta Descartes Peninsula (Fig. 2). The synonymy includes the following, previously used terms: Brito Fm., defined by Dengo (1962), and Cuajiniquil unit (Baumgartner et al. 1984).

Lithology and sedimentary structures

Originally, the Descartes Fm. was described as consisting of thin-bedded, tuffaceous, silts and fine- to coarse-grained sandstones alternating with breccias and conglomerates (Astorga 1987). However, reexamination in the study area revealed that the Descartes Fm. is composed of mm- to cm-sized turbiditic alternations. They consist of siliceous, hemipelagic mudstones and siltstones and lithic-arkosic, tuffaceous wackes and arenites that present a total thickness of 1800 m (Figs. 2, 3, 4, 5). The planktonic/pelagic fraction in the hemipelagic rocks is low (<20 %) and includes moderately preserved planktonic Foraminifera and radiolarians. The most common turbidites correspond to cm- to dm-sized, subtly graded, plane-parallel beds exhibiting Ta and Te interval couplets (Bouma 1962; Fig. 5). Generally, each bed contains several amalgamated turbiditic events (Fig. 5b, c). The grain size of the Ta intervals is generally comprised between silt and medium-grained sand, whereas the Te intervals correspond to siliceous hemipelagic mudstone and siltstone. Within one couplet, the Ta and Te intervals show different thicknesses, with one of the interval being systematically thicker than the other one. However, at the scale of the formation, the detrital-tuffaceous (Ta) and the hemipelagic (Te) sediments are present in equal proportions. Turbidites consisting of a more complete Bouma sequence are scarce and occur generally in 10 to 20-cm-thick beds.

In the upper part of the formation, a few turbidites contain small LBF that mark the base of Ta intervals (MZO1 and CR14-07; Figs. 4, 5d, 9). The input of these shallow-water organisms is concomitant with a general increase in the turbidite bed thickness. This trend is particularly well defined on the northern shore of the Bahia Cuajiniquil (N 10°57′11.1″/W 085°42′55.8″; Fig. 2), where dm- to m-bedded turbidites crop out below the limit with the overlying Junquillal Fm. These turbidites contain in places pebbles of volcanic rocks and shallow-water limestones with red algae and LBF that also occur in metric debris flows (roadside outcrop, now covered, located 2 km east of the Cuajiniquil village; Baumgartner et al. 1984).

On the Isla Juanilla (Fig. 2), the Descartes Fm. consists of a heterolithic facies (facies F1; Figs. 4, 5e, 7). This facies of the uppermost Descartes Fm. represents the oldest lithology observed on the Isla Juanilla. It crops out over a distance of 200 m (at low tide) and up to 50 m above sea level on the northern slope of the island, with an estimated thickness of 25 m. This brittle lithology is made of cm- to dm-bedded, greenish brown, silty mudstones alternating with centimetric, beige, arkosic wackes (Fig. 5e, f). The mudstones represent more than 80 % of the lithology. They are composed of hemipelagic, carbonate-bearing mud containing a low fraction of detrital minerals consisting of anhedral plagioclase crystals and opaque minerals (<10 %, 0.03–0.05 mm). The arkosic wackes are subtly graded and present a higher content in detrital minerals (15–17 % anhedral plagioclases; 7–9 % opaques; 0.04–0.2 mm, for both) and a carbonate matrix. Very rare planktonic Foraminifera are the only visible bioclasts. The sandy mudstone facies crops out also on the Isla Despensa (Figs. 2, 4, 5g) with a thickness of ~10 m and marks the transition from the fine-grained, turbidite facies of the Descartes Fm. to the amalgamated sandstones of the conformably overlying Junquillal Fm.

The submarine fan features interpreted from outcrops of the Punta Descartes (Astorga 1987) are actually tempestite deposits, now included with the overlying Junquillal Fm. Typical, coarse-grained, submarine channel complexes within the Descartes Fm. can be observed elsewhere in Costa Rica (SE Nicoya Peninsula; Astorga 1987) and Nicaragua (SW Nicaraguan Pacific coast; Struss et al. 2007).

Age of the Descartes Formation

The lowermost part of the formation exposed in Isla Los Cabros (Fig. 2) yielded planktonic Foraminifera species such as *Morozovella subbotinae* and *Globanomalina luxorensis*, which indicate a latest Thanetian–middle Ypresian age (sample Clr26 of Clerc 1998; Fig. 3). The co-occurrence of *Morozovella subbotinae* (range: latest Thanetian–middle Ypresian; Pearson et al. 2006) and *Turborotalia*
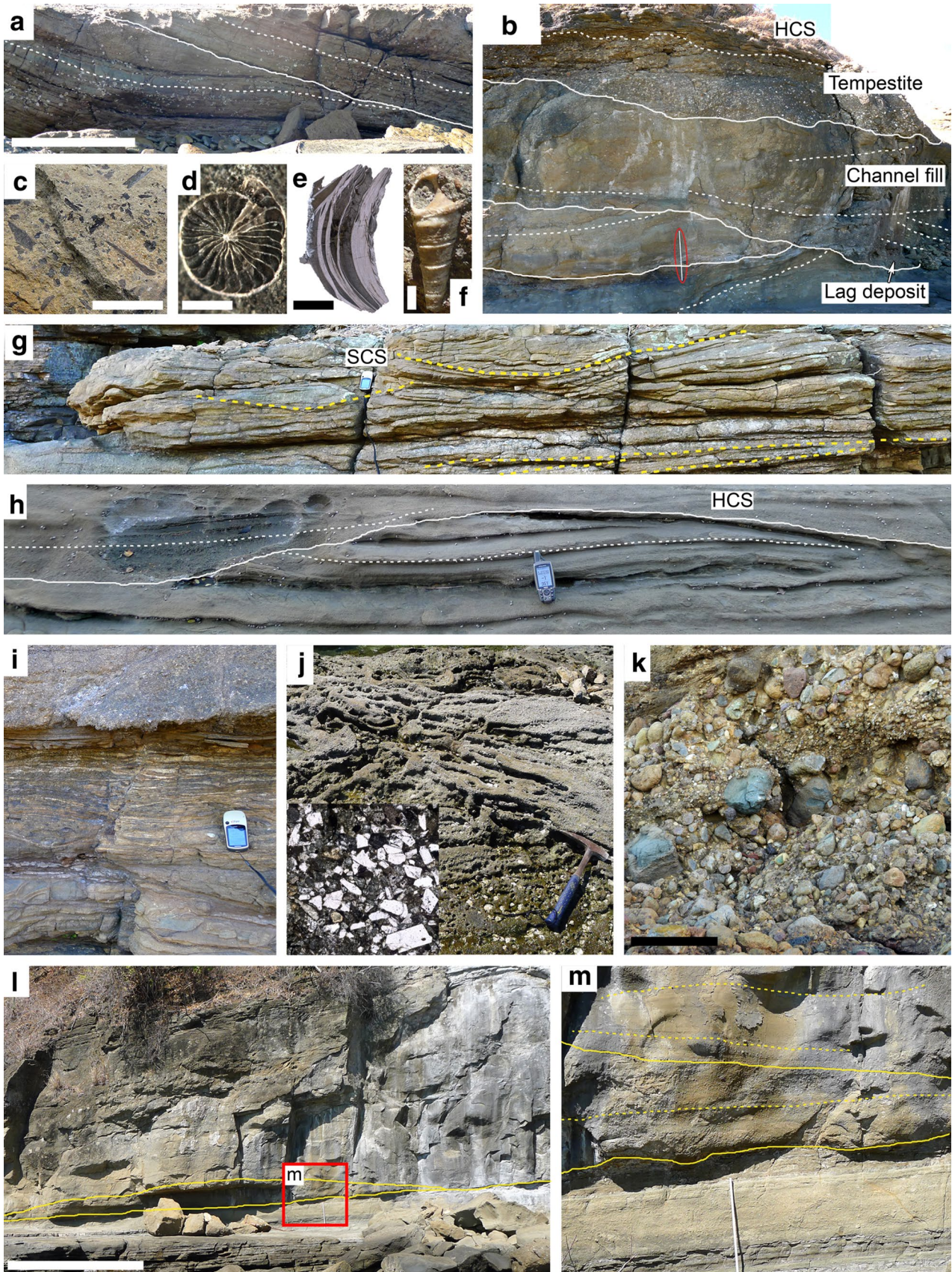
◄**Fig. 6** Field photographs of the upper Eocene Junquillal Fm. The *continuous lines* represent unconformities whereas the *dashed lines* underline the stratification. See Fig. 2 for locations. **a** Low-angle cross-stratification occurring in coarse-grained arenites (Playa El Coco, N 11°02′50.2″/W 085°43′52.4″). *Scale bar* 1 m. **b** Channel fill deposits unconformably overlain by tempestitic deposits (115 m SE of Punta Zacate, N 11°02′53.8″/W 085°43′37.8″). The channel fills show a basal lag deposit and unconformably overly planar-stratified arenites. The channel fill deposits present planar cross-stratifications prograding mainly to the *right*. The tempestite exhibits a basal clast-supported pebble conglomerate that grades into fine-grained arenites presenting hummocky cross-stratifications (*HCS*). *Double meter stick* 1 m. **c** Organic matter debris in a silty facies (Playa El Coco). *Scale bar* 1 cm. **d** Nummulitid shell (Bahia El Jobo southern shore). *Scale bar* 1 mm. **e** Thin-section photomicrograph of a centimetric bivalve shell (southern Punta Descartes). *Scale bar* 1 cm. **f** Gastropod shell (Playa Rajada). *Scale bar* 1 cm. **g** Finning-upward set of cross-strata (300 m SE of Punta Zacate, N 11°02′49.3″/W 085°43′30.0″). The *lower, coarse-grained part* shows low-angle cross-stratifications. The *upper, fine-grained part* displays swaley cross-stratifications (*SCS*) with concave-up strata. Length of the GPS device is 10 cm. **h** Hummocky cross-stratifications (*HCS*) developed in fine-grained arenites (Bahia El Jicote, N 10°57′36.3″/W 085°42′17.1″). *GPS device* length 14 cm. **i** Wavy-bedded heterolithic facies consisting of very fine-grained arenites (*bright color*) and silts (*dark color*), and encompassed between coarser deposits (390 m SE of the Punta Zacate, N 11°02′48.7″/W 085°43′29.1″). *GPS device* length 10 cm. **j** Cross-stratified, arkosic-lithic arenite (facies F2 in Fig. 7) occurring as boulders on the northern shore of the Isla Juanilla (N 10°59′00.5″/W 085°42′56.8″). *Hammer* length is 31 cm. The *lower left* insight shows a thin-section photomicrograph of the arenitic facies. Width of the image is 3.1 mm. **k** Unorganized deposits consisting of clast-supported, polymict conglomerates (Playa Rajada, N 11°02′39.5″/W 085°43′19.8″). *Scale bar* 1 m. **l** Submarine dunes comprised in massive, metric, stacked beds unconformably overlying centimetric siltstones (Playa El Jobo, N 11°02′19.2″/W 085°44′19.8″). *Scale bar* 5 m. **m** Close-up view of the outcrop shown in **l**. An erosive surface separates the submarine dunes from the underlying silty beds. The dunes grade from coarse-grained to fine-grained arenites and are characterized by low-angle cross-stratifications. *Double meter stick* length 0.8 m

praecentralis (range: middle Ypresian–late Lutetian; Blow 1979) indicates a middle Ypresian age for the underlying, uppermost Buenavista Fm. (sample Clr24 of Clerc 1998; Fig. 3). Consequently, the base of the Descartes Fm. is middle Ypresian (early Eocene) in age (by stratigraphic superposition).

The uppermost part of the formation (Playa Manzanillo; Fig. 2) yielded a LBF assemblage (samples MZO1 and CR14-07; Figs. 3, 4, 9) with the following species: *Nummulites floridensis* Heilprin, *Nummulites trinitatensis* (Nutall), *Amphistegina parvula* (Cushman), *Lepidocyclina* (*Nephrolepidina*) *chaperi* Lemoine and Douvillé, *Lepidocyclina pustulosa* H. Douvillé, and *Lepidocyclina ariana* Cole and Ponton. According to Frost and Langenheim (1974), Butterlin (1981), and Robinson and Wright (1993), this assemblage indicates a Priabonian (late Eocene) age. Recent investigations by Molina et al. (2016) found *Nummulites floridensis*, *Lepidocyclina chaperi*, *L. pustulosa* and orthophragminids in deep water sediments of Cuba,

associated with earliest Oligocene (Rupelian) planktonic Foraminifera and nannofossils (Ol, P18, NP21/CP16). Based on a review of data from Florida, Jamaica and the Tethyan realm, these authors conclude that the extinction of the orthophragminids may be diachronous and occur in the earliest Oligocene of the Caribbean and Tethyan realms. However, reworking of latest Priabonian faunas into lower Rupelian deep-water turbiditic sediments cannot be excluded, neither in the Cuban section or in the Descartes Fm., which therefore, may or may not reach into the lowest Oligocene. In the Brito Fm. (Nicaraguan equivalent of the Descartes Fm.), an early late Eocene age was obtained with planktonic Foraminifera and nannofossils (Struss et al. 2007).

Hence, the Descartes Fm. is of middle Ypresian to Priabonian (Eocene), perhaps to early Rupelian (Oligocene) age (Fig. 3).

Depositional environment

The lithologies of the Descartes Fm. were interpreted as basin plain volcaniclastic turbidites interstratified with submarine fan complexes, channel overbank deposits and slumps (Astorga 1987). In its type area, the Descartes Fm. shows exposures of thin-bedded, tuffaceous, fine-grained turbidites, which alternate with hemipelagic siliceous rocks containing planktonic Foraminifera and radiolarians. These thin alternations are indicative of a constant interplay between turbiditic and hemipelagic sedimentation in a deep-water environment. The distal character of the turbidites is attested by their limited thickness (mainly mm- to cm-thick), their grain-size (silt to medium-grained sand) and the high content of hemipelagic sediment, which is present in the same proportions as the turbiditic detrital fraction. Regarding our study, there are no paleobathymetric (faunal) indicators that would allow to ascertain precisely the water depth at which the turbidites deposited. Based on paleobathymetric data from well reports, Struss et al. (2008) estimate a paleo-water depth of 3000 m for the Brito Fm. (Nicaragua). Mutti et al. (2007) indicate that most of the modern turbidite systems develop at depths in excess of 1000 m. Moreover, such depths are commonly inferred for ancient examples.

In the uppermost part of the formation, the input of platform-derived clasts associated with a thickening- and coarsening-upwards of the turbidites evidence an increasing proximality of the turbiditic system that precedes the onset of shelf sedimentation. Similarly, the heterolithic lithologies of the Descartes Fm., which are exposed on the Isla Juanilla (Fig. 5e) and on the Isla Despensa (Figs. 4, 5g) represent a rather proximal, offshore facies. These sediments deposited in a low-energy environment that marks a regression between the deep-water deposits of the Descartes Fm.
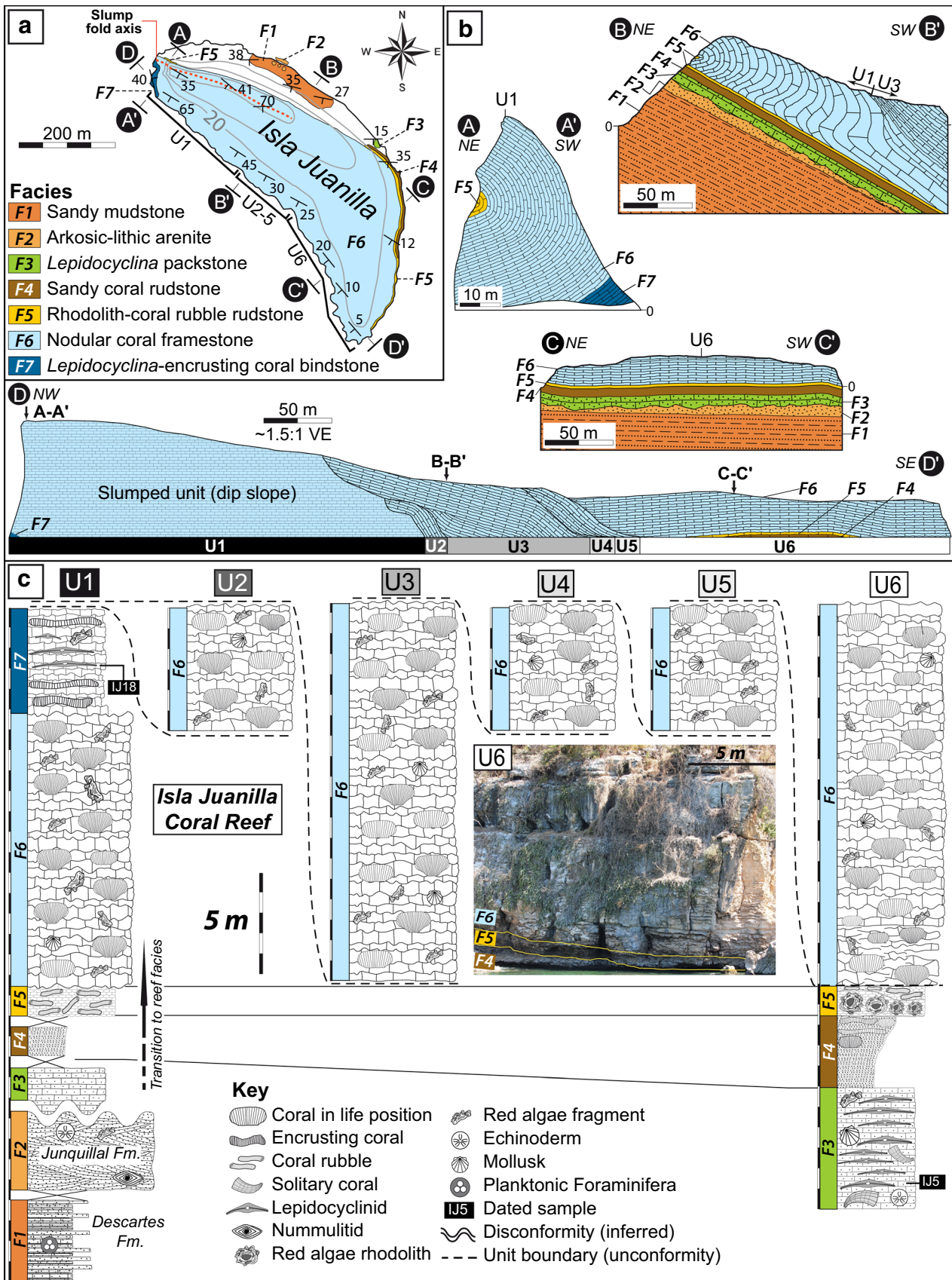
a

Slump fold axis

Facies
F1	Sandy mudstone
F2	Arkosic-lithic arenite
F3	*Lepidocyclina* packstone
F4	Sandy coral rudstone
F5	Rhodolith-coral rubble rudstone
F6	Nodular coral framestone
F7	*Lepidocyclina*-encrusting coral bindstone

Isla Juanilla

b

c

U1 U2 U3 U4 U5 U6

Isla Juanilla Coral Reef

5 m

Transition to reef facies

Junquillal Fm.

Descartes Fm.

Key
- Coral in life position
- Encrusting coral
- Coral rubble
- Solitary coral
- Lepidocyclinid
- Nummulitid
- Red algae rhodolith
- Red algae fragment
- Echinoderm
- Mollusk
- Planktonic Foraminifera
- **IJ5** Dated sample
- Disconformity (inferred)
- Unit boundary (unconformity)

◄**Fig. 7** Geology, structure and stratigraphic architecture of the upper Oligocene Juanilla Formation. **a** Facies map of the Isla Juanilla displaying the seven facies recognized in the field and described in the text (*F1* = Descartes Fm.; *F2* = Junquillal Fm.; *F3–F7* = Juanilla Fm.). The cross-section transect positions are indicated by *A–A'*, *B–B'*, *C–C'* and *D–D'*, and shown in **b**. **b** Cross sections of the Isla Juanilla. *A–A'*: NE–SW-oriented cross-section (no vertical exaggeration) of the Isla Juanilla northwestern corner exhibiting a recumbent fold. *B–B'*: NE–SW-oriented cross section (no vertical exaggeration) of the Isla Juanilla central part. *C–C'*: NE–SW-oriented cross section (no vertical exaggeration) of the Isla Juanilla southern part. *D–D'*: NW–SE-oriented cross section (1.5:1 vertical exaggeration) of the WSW Isla Juanilla shore. This cross section shows the Isla Juanilla Coral Reef internal architecture, which consists of six distinct units (*U1–U6*). **c** Stratigraphic logs of the six coral reef units (*U1–U6*) depicted in **b** (*D–D'*). The fossil content is not exhaustive and only the most common fossils are depicted. The unit *U1* represents the oldest part of the Isla Juanilla Coral Reef

and the siliciclastic shelf deposits of the Junquillal Fm. The latter is marked by the appearance of massive, amalgamated arenites.

Junquillal Formation: a new lithostratigraphic unit

The Junquillal Fm. is herein defined as a new formal lithostratigraphic unit which consists of outcrops located between the Bahia Cuajiniquil northern shore and the Bahia Salinas northern shore (type area; Fig. 2). The definition of the Junquillal Fm. proposed hereafter includes the Junquillal unit of Baumgartner et al. (1984). Its definition is based on a sedimentologic, stratigraphic and biostratigraphic study of the exposures described below. These outcrops were previously considered as part of the Descartes Fm. (Astorga 1987). However, the detailed study of the outcrops reveals shallow shelfal characteristics that are incompatible with an assignment to the deep-water, turbiditic Descartes Fm.

Stratotype and reference sections

The holostratotype section is located on the Isla Despensa (Figs. 2, 4). The base of the 25-m-thick section is situated on the southern end of the island's inner beach (Fig. 5g). The Isla Despensa section is established as the holostratotype section for the following reasons: (1) the exposed lithologies are characteristic of the newly defined lithostratigraphic unit, (2) the clear stratigraphic relationship with the underlying Descartes Fm., and (3) the conspicuous facies difference with the underlying Descartes Fm., as defined above.

Well-preserved outcrops of the Junquillal Fm. are continuously exposed on the western shore of Punta Descartes, and between the northern shore of the Bahia Cuajiniquil and the southern shore of the Bahia Junquillal (Fig. 2). Within these exposures, three parastratotype sections are

established in order to additionally characterize the Junquillal Fm. (Figs. 4, 6): (1) a 40-m-thick section located at the Playa El Coco, (2) a 20-m-thick section located at the Playa Rajada, and (3) a 7-m-thick section located 115 m southeast of the Punta Zacate.

Formation boundaries

The lower boundary is equivalent to the Descartes Fm. upper boundary defined above.

A cryptic upper boundary with the Juanilla Fm. is tentatively established on the northern Isla Juanilla (N 10°59′00.5″/W 085°42′56.8″; Figs. 2, 7a). However, the Juanilla Fm. rests unconformably on the deeply eroded Junquillal Fm., in view of its reduced thickness outcropping on the island (Figs. 4, 7c). The contact has not been observed directly, but it is deduced from the occurrence of unconformable outcrops of Junquillal lithologies between the Descartes and the Juanilla outcrops (Fig. 6j).

Derivation of the name and synonymy

The formation is named after the Bahia Junquillal (Fig. 2). The synonymy includes the following, previously used terms: part of Brito Fm., defined by Dengo (1962), Junquillal unit (Baumgartner et al. 1984), and part of Descartes Fm. (Astorga 1987; Denyer and Alvarado 2007).

Lithology and sedimentary structures

General features The Junquillal Fm. is defined as a siliciclastic shelf deposit which crops out on the coasts of the Bahia Junquillal and the Punta Descartes, as well as on the Isla Despensa and Isla Juanilla (Fig. 2). The formation consists mainly of medium- to coarse-grained, amalgamated sandstones which alternate in places with lenses and beds of granule to pebble and locally boulder conglomerates with a sandy matrix. These lithologies are typically comprised in large-scale, low-angle to high-angle cross-stratified beds (Fig. 6). The Junquillal Fm. exhibits numerous fining-upwards, metric tempestites. They consist of a basal, lag deposit, composed of massive conglomerates with rip-up clasts resting in general on a scoured surface and grading upsection into coarse-grained arenites. The basal lag deposits are overlain by fine-grained arenites showing hummocky cross-stratification (HCS) and which can be in turn overlain by very thin-bedded, fine-grained sand- and siltstones. Large-scale, low-angle cross-stratification is observed in the basal coarse-grained deposits of the tempestites. These features are present in the stratotype sections (Fig. 4). Pelites are almost absent from the Junquillal Fm. and correspond to sandy/silty mudstones when they crop out. Based on the geological map (Fig. 2),
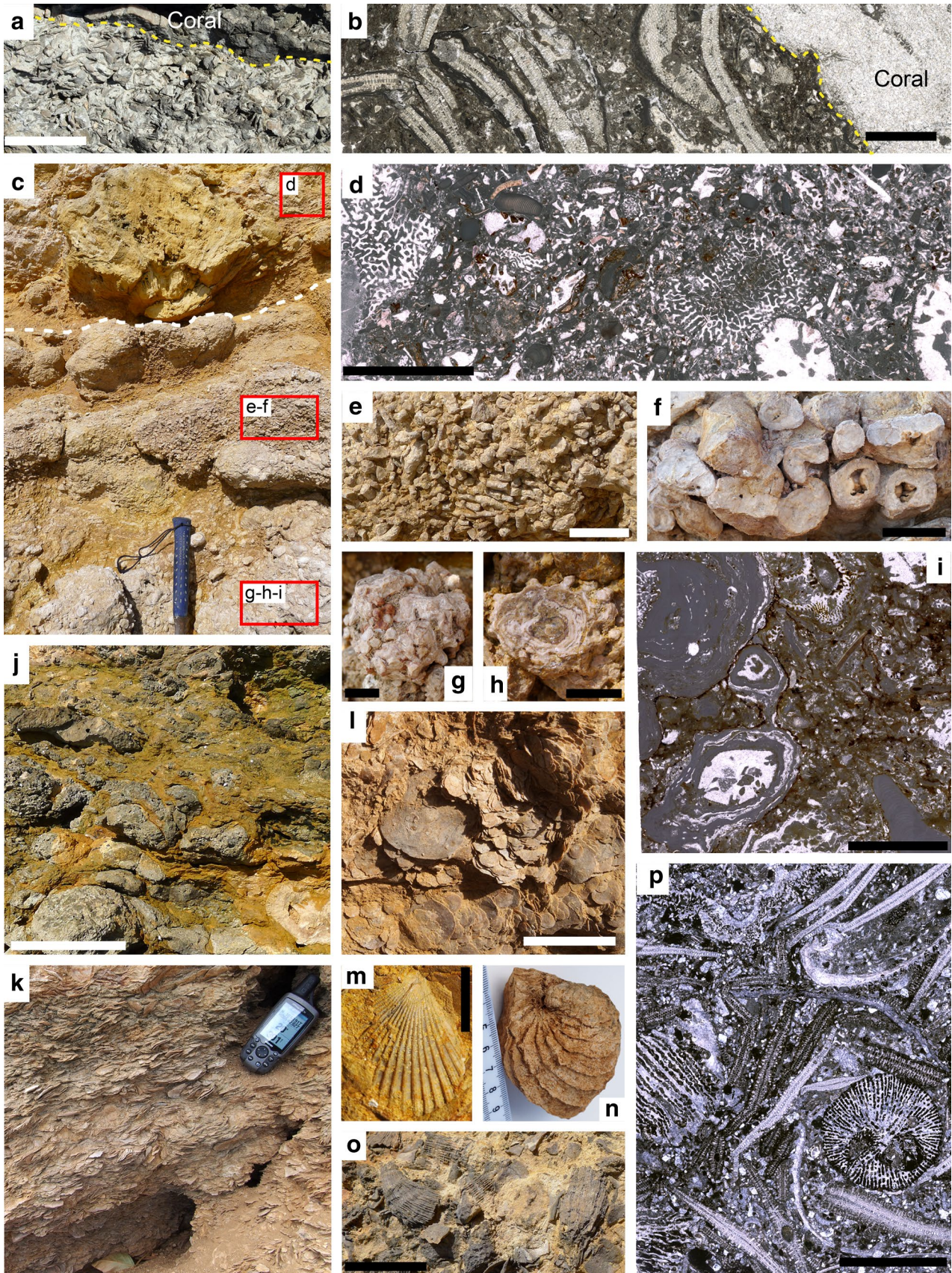
◀ **Fig. 8** Field photographs and thin-section photomicrographs of the upper Oligocene Juanilla Formation. **a** Close-up view of the *Lepidocyclina*-encrusting coral bindstone facies (F7) (N 10°58′59.0″/W 085°43′05.0″). *Scale bar* 5 cm. **b** Thin-section photomicrograph of the *Lepidocyclina*-encrusting coral bindstone facies (F7) shown in **a**. *Scale bar* 5 mm. **c** Outcrop exhibiting the rhodolith-coral rubble rudstone facies (F5) overlain by the nodular coral framestone facies (F6) (N 10°58′48.9″/W 085°42′48.8″). The contact is highlighted with a *dashed line*. *Hammer* length 21 cm. **d** Thin-section photomicrograph of the nodular coral framestone facies (F6). *Scale bar* 5 mm. **e**–**h** Close-up views of the rhodolith-coral rubble rudstone facies (F5). Same outcrop as in **c**. **e** Coral rubble consisting of branching coral debris. *Scale bar* 2 cm. **f** Coherent coral framework within the rubble. *Scale bar* 5 cm. **g**, **h** Centimetric warty rhodoliths displaying spheroidal (**g**) and ellipsoidal (**h**) shapes. *Scale bars* 1 cm. **i** Thin-section photomicrograph of the rhodolith-rich part of the rudstone facies (F5) shown in **c**. *Scale bar* 5 mm. **j** Sandy coral rudstone facies (F4) exhibiting encrusting and domal corals embedded in a detrital wackestone matrix. Same outcrop as in **c**. *Scale bar* 20 cm. **k**–**p** *Lepidocyclina* packstone facies (F3) (N 10°58′54.9″/W 085°42′49.9″). **k** Moderately packed accumulation of *Lepidocyclina* tests aligned parallel to the bedding. *GPS device* length 14 cm. **l** Close-up equatorial view of the discoidal *Lepidocyclina* tests shown in **k**. *Scale bar* 5 cm. **m**, **n** Bivalve shells. **m** *Scale bar* 1 cm. **n** Note the *double meter stick* for scale. **o** Centimetric horn-shaped, solitary corals. *Scale bar* 2 cm. **p** Thin-section photomicrograph of the *Lepidocyclina* packstone facies (F3) displaying lepidocyclinids, bivalve shell debris and solitary coral fragments. *Scale bar* 5 mm

the apparent thickness of the Junquillal Fm. is comprised between 2000 and 2200 m. The described sections share common lithological characteristics, therefore microfacies details are given only for one locality, the Playa El Coco section (Fig. 4).

Isla Despensa section (*holostratotype*) The Isla Despensa (Fig. 2) displays a 20-m-thick section consisting of cm-bedded, fine- to coarse-grained arenites alternating with dm- to m-bedded granule and pebble conglomerates (Fig. 4). The base of the section is made of 10 m of fine- to medium-grained arenites which show occurrences of HCS. These arenites are unconformably overlain by a fining-upward, 5-m-thick tempestite which grades from a basal pebble conglomerate into a hummocky cross-stratified arenitic bed at the top. The tempestite is unconformably overlain by a massive, 8-m-thick succession of metric, stacked channel deposits made of granule and pebble conglomerates.

Playa El Coco section The Playa El Coco (Fig. 2) western shore displays a 40-m-thick section (Fig. 4) composed of cm- to dm-bedded sandstones. The sandstones correspond to lithic-arkosic wackes and arenites compounded of moderately to moderately well sorted, subrounded to rounded elements. Volcaniclastic lithoclasts represent generally the dominant rock constituent (25–45 %, 0.5–1.5 mm), although they are almost absent from the most fine-grained lithologies. Scarce sedimentary lithoclasts include sand- to pebble-sized clasts of radiolarite, pelagic limestone and platform limestone. In few beds, pebbles

and rare cobbles appear in ungraded, granule conglomerate lenses. Detrital minerals correspond to fine- to coarse-grained sands. Anhedral to subeuhedral plagioclase crystals are the most common mineralogical elements (15–30 %). Anhedral opaque minerals also account for a significant rock fraction (10–12 %). Green pyroxene and amphibole minerals correspond to a minor component (<5 %). Bioclasts are rare and include mm- to cm-sized LBF, mollusk shells and corals. The sample COC5 yielded datable LBF (Fig. 9a). Wood-rich layers are commonly encountered (Fig. 6c). Sedimentary structures are observed in several places and comprise HCS, swaley cross-stratifications (SCS) and high-angle cross-stratifications. HCS and SCS developed in fine-grained sandstones and are composed of low-angle, centimetric, curved beds. The angle between the beds and erosional truncations is low, with the overlying beds being parallel to the erosional surface. The structures have amplitudes of 0.3–0.4 m and wavelengths between 0.9 and 2 m. A 3-m-thick conglomerate deposit rests with an erosive base on finer lithologies in the upper part of the section. Well-preserved nummulitids and lepidocyclinids as well as cm-sized bivalve shells are widespread in the conglomerate matrix.

Punta Zacate area Cross-stratification features are visible in the outcrops located 115 m southeast of the Punta Zacate (Fig. 2). There, large-scale, planar cross-stratification structures developed in coarse arenites and matrix-supported, polymict, pebble conglomerates interpreted as stacked channel fill deposits (Figs. 4, 6b). The base of the 5-m-thick coset consists of a structureless, lag deposit containing cobbles and rare boulders. A part of the coset locally overlies a centimetric bed which shows occurrence of wavy bedding structures. Generally, the conglomeratic channel deposits are stacked and no finer-grained deposits are preserved. The dm- to m-thick sets are separated by truncation surfaces and the different sets show variable strata angles between them, sometimes with opposite dip directions. Strata can be followed laterally over distances up to 10 m and are generally well defined in cases where different grain sizes alternate. The channel fill deposits are overlain by a 2-m-thick tempestitic deposit made of a basal, massive, lenticular conglomeratic bed with an erosional base which grades into fine-grained, cm-bedded sandstones presenting HCS structures.

SCS structures are present 300 m southeast of the Punta Zacate (Figs. 2, 6g). In one locality situated 390 m southeast of the Punta Zacate (Fig. 2), wavy bedding structures appear within a 40-cm-thick bed made of mm- to cm-sized alternations of sandy and silty sediments (Fig. 6i).

Playa Rajada section Clast-supported, polymict conglomerates crop out in an 18-m-thick section located on the northwestern Playa Rajada (Figs. 2, 4, 6k). These metric beds are composed of a cobble-sized, moderately sorted
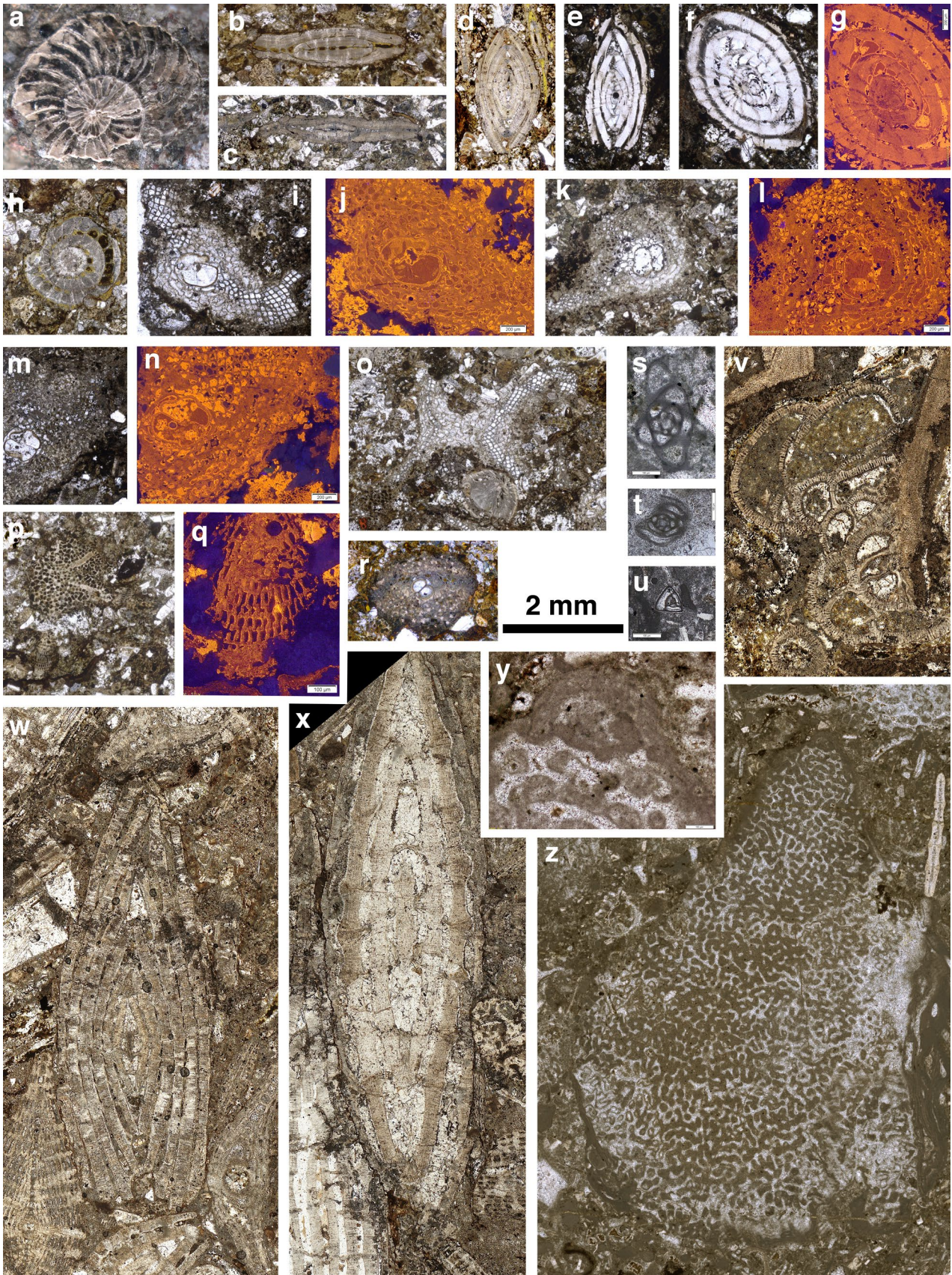
◀**Fig. 9** Larger Benthic Foraminifera of the Descartes (**b–r**) and Junquillal Formations (**a**, **s–z**). Figures are light microscopic images, and optical cathodoluminescence images (CL), where indicated. *Scale bar* is 2 mm unless indicated otherwise. **a–c** *Nummulites floridensis* Heilprin. **d–g** *Amphistegina parvula* (Cushman). **g** CL. *Scale bar* 200 μm. **h** *Nummulites trinitatensis* (Nutall). **i–l** *Lepidocyclina pustulosa* H. Douvillé. **j, l** CL. *Scale bar* 200 μm. **m, n** *Lepidocyclina* (*Pliolepidina*) cf. *pustulosa*. **n** CL. *Scale bar* 200 μm. **o**. *Lepidocyclina chaperi* Lemoine and Douvillé (stellate form). **p, q** *Asterocyclina* cf. *asterisca*. **q** Detail under CL showing the equatorial layers in a ribbed fragment. *Scale bar* 200 μm. **r** *Lepidocyclina ariana* Cole and Ponton. **s–u** Miliolids. *Scale bar* 10 μm. **s** *Quinqueloculina* sp. **t** Miliolid. **u** *Triloculina* sp. **v** *Victiorella* sp. **w** *Nummulites striatoreticulatus*. **x** *Operculinoides kugleri*. **y, z** *Dictyoconus* sp. **y** apical part of *Dictyoconus* sp. *Scale bar* 100 μm. **a** Sample COC5 (Playa El Coco); **b, c** Sample MZO1 (Playa Manzanillo); **d–r** Sample CR14-07 (Playa Manzanillo); **s–u, y, z** Sample CR14-10 (Playa Rajada); **v–x** Sample 1529 (Bahia Junquillal). See Figs. 2 and 4 for locations and GPS coordinates

matrix which contains randomly scattered boulders (diameters: 0.3–0.8 m). The majority of the clasts originate from various differentiated volcanic lithologies. Scarce sedimentary clasts correspond to shallow-water limestones often containing lepidocyclinids, asterocyclinids, *Dicytioconus* sp., and few miliolids, such as *Quinqueloculina* sp. (CR14-10; Fig. 9). The clast-supported, polymict conglomerates alternate with arenites and pebble-sized, matrix-supported conglomerates.

Isla Juanilla The Junquillal Fm. is only observed as boulders of arkosic-lithic arenites fallen from the northern slope of the island and which contain a few fragments of LBF, red algae and echinoderms (facies F2; Figs. 6j, 7). Its thickness on the island is probably less than 10 m (Figs. 4, 7). The sedimentary contact with the thin-bedded turbidites (facies F1) of the underlying Descartes Fm. has not been directly observed.

Other sections HCS developed in the most fine-grained deposits of the Bahia El Jicote and Bahia Junquillal outcrops (Figs. 2, 6h). Large-scale, low-angle cross-stratifications are present in the outcrops of the Bahia Jobo shores (Fig. 2). In both localities, these structures developed in medium to coarse-grained arenites comprised in submarine dune sets which present metric heights and pluri-metric widths (Fig. 6l, m). Carbonate beds rich in LBF have been encountered in the outcrops of the Bahia Junquillal southwestern shore (1529, N 10°57′49.9″/W 085°41′47.6″; Fig. 10).

Age of the Junquillal Formation

During our fieldwork, several LBF-bearing samples were collected (Figs. 9, 10). The sample COC5 from the Playa El Coco contains an individual open spiral form as in *Operculinoides* Hanzawa (Fig. 9). In the sample 1529 (Bahia Junquillal, N 10°57′49.9″/W 085°41′47.6″;

Fig. 10), we determined *Lepidocyclina* (*Nephrolepidina*) *chaperi* Lemoine and Douvillé, *Lepidocyclina* (*Nephrolepidina*) *macdonaldi* Cushman, *Lepidocyclina ariana* Cole and Ponton, *Lepidocyclina pustulosa* H. Douvillé, *Fabiania* A. Silvestri in fragments, *Nummulites willcoxi* Heilprin, *Nummulites striatoreticulatus* L. Rutten, *Asterocyclina asterisca* (Guppy), *Asterocyclina* sp., *Discocyclina* sp. and fragments of *Heterostegina* sp. Even if some of these species have their first occurrence in the middle Eocene, the presence of *Lepidocyclina chaperi* indicates a Priabonian age according to Frost and Langenheim (1974), Butterlin (1981), and Robinson and Wright (1993). More recently, Molina et al. (2016) concluded that some forms may have survived until the early Oligocene (see remarks under age of the Descartes Fm. above). On the other hand, reworking of LBF from Priabonian strata cannot be excluded. Therefore the Junquillal Fm. may reach into the earliest Oligocene.

Depositional environment

The facies succession observed from the top of the Descartes Fm. through the Junquillal Fm. (Figs. 4, 5, 6) is characterized by shallowing-upward conditions that recorded a rapid regression. The lithologies of the Bahia Cuajiniquil northern shore and the roadside outcrops west of the Cuajiniquil village (Fig. 2) clearly show the rapid transition from Descartes Fm. distal facies to the shallow shelf facies of the Junquillal Fm. This transition occurs within a few meters and is accompanied by the input of relatively coarser, platform bioclast-rich sands and platform-derived pebbles preceding the onset of shelf, siliciclastic sedimentation.

The different sections of the Junquillal Fm. are characterized by amalgamated storm deposits that take the form of fining-upward tempestites. The tempestites comprise three facies that correspond, from base to top, to poorly stratified basal conglomerates, hummocky-stratified fine-grained arenites and flat-bedded silts which are rarely preserved. This facies succession records one or several storm events of which the peak energy is illustrated by the deposition of the conglomeratic lag bed that may be the result of multiple winnowing events. Lag deposits are overlain by HCS structures that formed during the waning stage of the last event. The overlying thin-bedded silts correspond to suspension fallout during fair weather conditions occurring between the storms. The HCS and SCS structures observed in the Junquillal Fm. are indicative of storm-influenced, shelf environments (Dott and Bourgeois 1982; Walker et al. 1983; Duke 1985; Cheel and Leckie 1993; Dumas and Arnott 2006). Also, the development of large-scale, low-angle to high-angle cross-stratifications suggests the deposition under the influence of multi-directional currents and
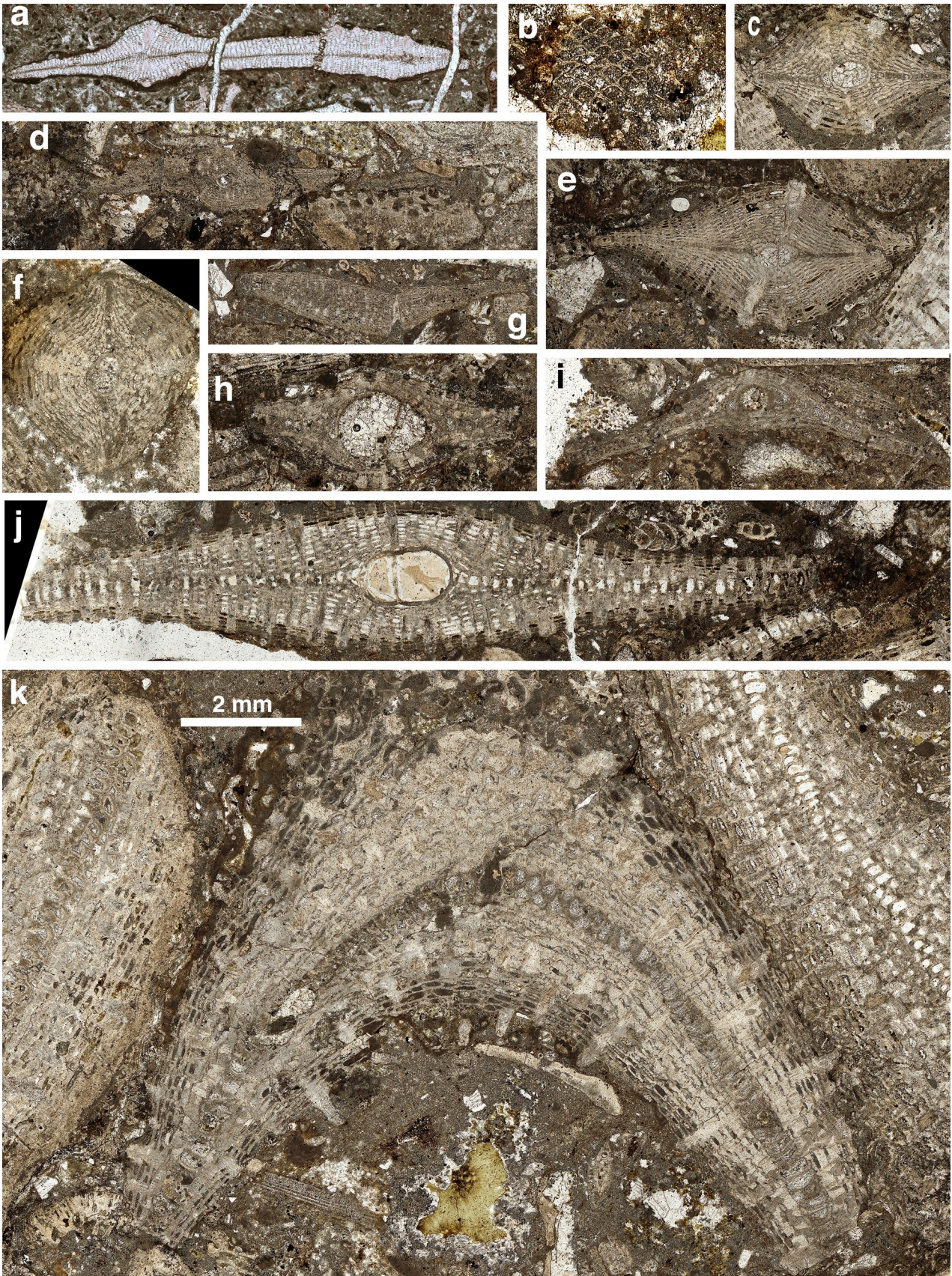
◄**Fig. 10** Larger Benthic Foraminifera of the Junquillal Formation. All figures are light microscopic images. *Scale bar* is 2 mm for all figures, except for **b**, which is 1 mm. **a** *Asterocyclina* cf. *marianensis* (Cushman). Vertical oblique section showing 18 lateral chambers on each side of the median plane. **b** Fragments of the ogival equatorial chambers probably of *Lepidocyclina pustulosa* (H. Douvillé). **c** *Lepidocyclina pustulosa* (H. Douvillé), central vertical section of megalospheric form of a small specimen. **d** *Discocyclina* sp. Vertical oblique section of megalospheric specimen with 12 lateral chambers arranged in regular tiers fragment showing the ribbed form in the distal part. **e, f** *Lepidocyclina* (*Lepidocyclina*) *pustulosa* (H. Douvillé). **e** Central vertical section of megalospheric form with a pronounced umbo and thin flange. **f** Central vertical section of megalospheric form showing the embryonic chambers in an inflated specimen. **g** *Discocyclina* sp. **h** *Lepidocyclina ariana* Cole and Ponton. Eroded vertical, oblique section of a megalospheric form. The equatorial layers in the vertical plane are observed near the protoconch side. The lateral chambers are straight and thick. **i** *Lepidocyclina* cf. *chaperi*. **j** *Lepidocyclina* (*Lepidocyclina*) *macdonaldi* Cushman. Vertical section of megalospheric form showing the embryonic chambers, the pillars and the thick open roofs and floors of lateral chambers. **k** *Lepidocyclina chaperi* Lemoine and Douvillé. Oblique section of saddle-shaped specimen. **a** Sample CR14-10 (Playa Rajada); **b–k** Sample 1529 (Bahia Junquillal). See Figs. 2 and 4 for locations and GPS coordinates

waves in shoreface conditions (Ricci Lucchi 1995; Dumas and Arnott 2006; Santra et al. 2013).

The metric, stacked conglomeratic deposits observed at the Punta Zacate (Figs. 2, 4) are interpreted as the results of lateral migration of channels which produced beds presenting planar cross-stratifications with opposite bed dip angles (Fig. 6b).

The local occurrence of boulder-bearing, clast-supported conglomerates (Playa Rajada, Punta Descartes; Figs. 2, 6k) is interpreted as the result of submarine, rock avalanche deposits in the vicinity of a river or delta mouth. Prior to the avalanching process, the clasts were rounded in a fluviatile and/or beach environment and subsequently deposited in the nearshore area, close to a river mouth (small Gilbert type delta?). Given the absence of matrix and the poor sorting, the cobbles and the boulders were finally transported and mixed in a rock avalanche by gravity, possibly triggered by storm events or flood events in the river system, as well as earthquakes.

The general absence of mud- to silt-sized particles in the Junquillal Fm. is the consequence of continuous influence of high-energy currents and/or wave action. Consequently, the finest sediments remained suspended and were winnowed towards more distal, offshore settings. In the rare cases where fine-grained sediments have been preserved, it is possible to observe wavy bedding structures (Fig. 6i), which are typical in environments where higher and lower energy conditions alternate.

In conclusion, the studied tempestite facies suggest that the Junquillal Fm. deposited at or above the storm-wave base (SWB) in a proximal shelf (Myrow 1992; Einsele 2000). Indeed, it is not possible to ascertain the depths reached by the upper Eocene storms. In modern settings, the depth of the SWB can be very variable. However, it does not exceed 200 m (Immenhauser 2009). Regarding the modern eastern Pacific, Clifton (1988) estimated a depth of 150 m for the SWB on the central California shelf.

The proposed facies interpretation is in contradiction with the previous studies of the Punta Descartes-Bahia Junquillal area published by Astorga (1987, 1988), Winsemann and Seyfried (1991) and Winsemann (1992). The mentioned authors interpreted these deposits as multicycle fan complexes deposited in basinal environments. Their facies description pointed out the presence of channelized lobes interstratified with channel overbank deposits and basinal plain turbidites. However, deep-water facies have not been observed in the area coinciding with the Junquillal Fm. outcrops.

Juanilla Formation: a new lithostratigraphic unit

The Juanilla Fm. corresponds to an ancient carbonate platform exposure which has not been described or mentioned in the literature. This exposure represents a geographically limited, formal lithostratigraphic unit, given that it is restricted to the Isla Juanilla (~0.2 km^2; Figs. 2, 7). The Juanilla Fm. does not present a lateral continuity mappable at a regional scale. Therefore, the description of the Juanilla Fm. does not follow the same scheme as the previously described formations. The type area, the type section and the reference sections are comprised within the geographical extent of the Isla Juanilla (Figs. 2, 7). The lower boundary of the formation is equivalent to the upper boundary of the Junquillal Fm. (defined above).

On the Isla Juanilla, field investigations permitted to distinguish the three formations discussed here comprising seven different facies, with an estimated thickness of approximately 50 m (Figs. 7, 8). The facies F1 is part of the uppermost Descartes Fm., whereas the facies F2 is part of the Junquillal Fm. These facies have been described in the previous parts (Figs. 5, 6). The facies F3 to F7 compose the Juanilla Fm. (upper Oligocene; Figs. 7, 8). The facies F3-F4-F5 are considered as a pre-reef, platform facies association. The facies F6-F7 are defined as the Isla Juanilla Coral Reef.

Stratigraphic architecture of the Isla Juanilla Coral Reef

The dominant facies (F6) of the Juanilla Fm. corresponds to well-bedded, nodular, coral framestones (Figs. 7, 8c). The facies F6, along with the facies F7, represent the Isla Juanilla Coral Reef which deposited over a substratum made of the facies F3 to F5. The Isla Juanilla Fm. unconformably overlies the Junquillal and Descartes fms. (facies F1 and F2; Fig. 7b). The reef facies F6 occurs in six different stratigraphic units (U1 to U6; Fig. 7). In addition,
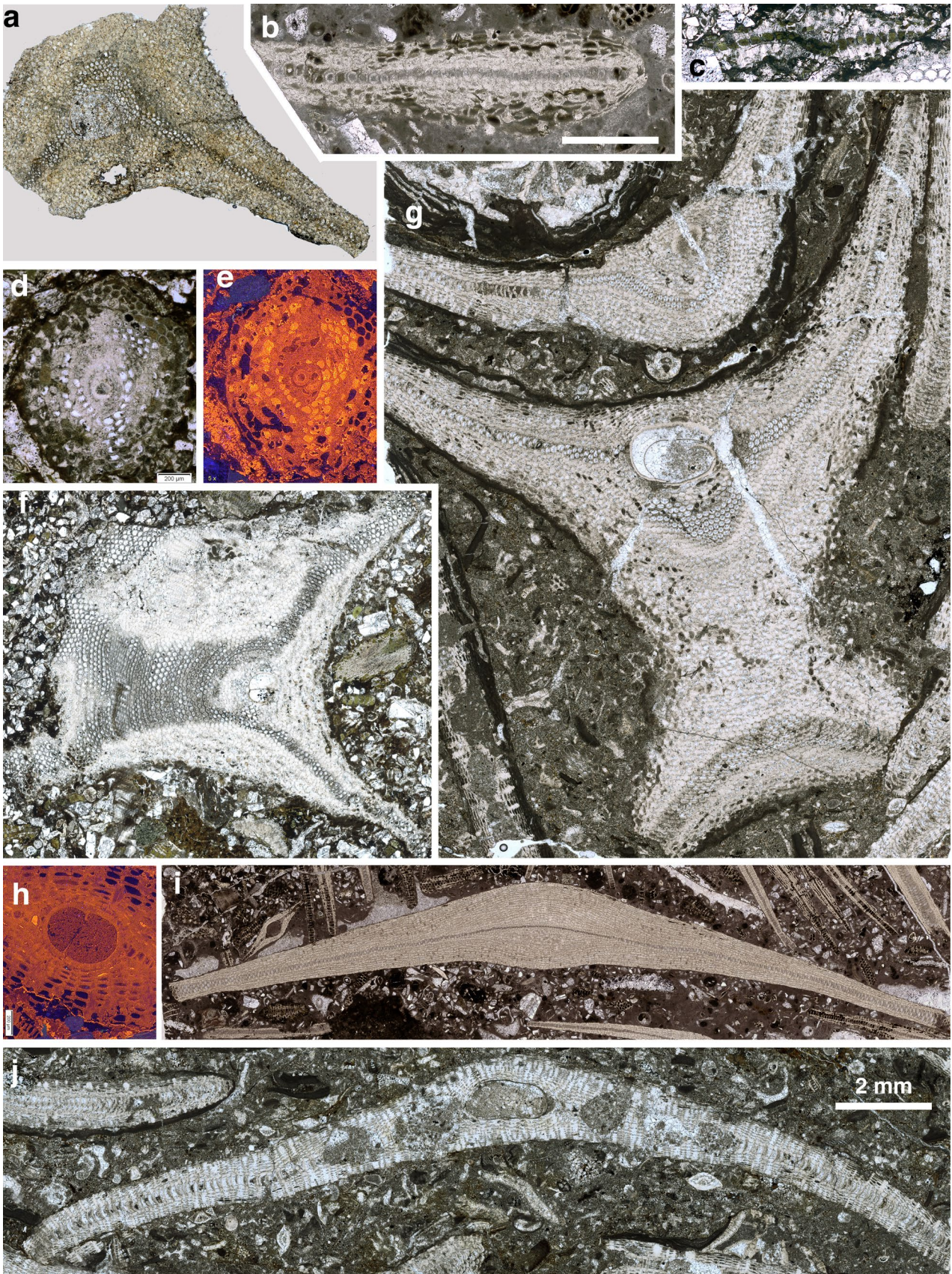
◀**Fig. 11** Larger Benthic Foraminifera of the Juanilla Formation. Figures are light microscopic images, and optical cathodoluminescence images (CL), where indicated. *Scale bar* is 2 mm, unless indicated otherwise. **a** *Lepidocyclina (Nephrolepidina) vaughani* Vaughan and Cole. **b** *Miolepidocyclina* cf. *panamensis*. *Scale bar* 1 mm. **c** *Miogypsinoides* sp. **d**, **e** *Helicosteginoides* sp. *Scale bar* 200 μm. **e** CL. **f** *Lepidocyclina foresti* Vaughan. **g** *Lepidocyclina (Eulepidina) favosa* Cushman. **h** *Lepidocyclina canellei* Lemoine and Douvillé. CL. *Scale bar* 200 μm. **i** *Lepidocyclina undosa* Cushman. **j** *Lepidocyclina (Eulepidina) favosa* Cushman. **a–f**, **h**, **i** Sample IJ5 (facies F3; Figs. 7, 8); **g**, **j** Sample IJ18 (facies F7; Figs. 7, 8)

the facies F7 is present only in the unit U1 (Fig. 7). The sedimentary structure of the six units is well exposed in the cliffs of the western-southwestern coast (Fig. 7a). There, a 700-m-long outcrop gives an insight to the reef growth (profile D–D'; Fig. 7b). In the central part of this section, the reef growth occurred towards the S–SE, through a series of steeply inclined, sigmoidal clinoforms. These clinoforms are distributed in four distinct, prograding units (U2 to U5) which onlapped an initial, slumped unit (U1, reef core). The sedimentary structure of the oldest unit is not easily observed on the northwestern shore as this zone of the island is strongly folded and corresponds to a dip slope. The first prograding unit (U2) is 6 m thick (topset dip angle = 30°; foreset = 60°). The following prograding unit (U3) is 80 m long and 20 m thick (topset = 20°; foreset = 40°). The last two prograding units (U4 and U5) are ~5 m thick, each, and exhibit well-developed sigmoidal clinoforms (foreset = 40°). The unit's U4 foreset and the unit's U5 bottomset downlap the unit's U3 bottomset. Finally, the southern part of the coral reef section (230 m long, 20 m thick) is included within an aggrading unit (U6) which onlaps the unit U5. In summary, the oldest rocks of the Isla Juanilla Coral Reef are located in the western-northwestern part of the island. This area corresponds to the initial unit (U1) from which the reef developed through four prograding units (U2 to U5) and finally one aggrading unit (U6).

Facies F3: Lepidocyclina packstone

A foraminiferal limestone (F3) is observed solely in a small outcrop of ~25 m^2 located on the eastern part of the Isla Juanilla (Fig. 7a). The limestone presents a pale blue-green fresh surface which derives from the mud-sized matrix and progressively alters to a brown patina. The outcrop shows a moderately packed accumulation of lepidocyclinids (35–60 % of the rock volume; Fig. 8k) which displays undulated, discoidal tests with mm- to cm-sized diameters (up to 6 cm) and thicknesses smaller than 4 mm (Figs. 8l, 11). The thickness/diameter ratio of the measured tests is comprised between 0.05 and 0.12. The foraminifers are generally accumulated with their major axis aligned parallel to

the bedding. The large lepidocyclinid tests, especially their rims, are easily broken due to their small thickness, hence they are not always entirely preserved. Apart from a large proportion of LBF, the limestone contains well-preserved centimetric tests of conical-shaped solitary corals and a few Pectinid and other bivalve shells (Fig. 8m–o). The solitary corals are randomly scattered in the sediment and do not occur in growth positions (Fig. 8o). Rare hermatypic corals and very flat, irregular echinoids ("sand dollar") also occur. The relation between the foraminiferal limestone and the overlying facies cannot be observed because of a 1 m-gap in the outcrop.

The microfacies analysis allows the following observations. Smaller benthic foraminifers are frequent in the matrix (3–5 %, 0.2–0.6 mm). Mollusk shells and debris are common constituents (5–9 %, 0.5–9 mm). Subangular, poorly sorted calcitic debris are widespread (6–9 %, 0.1–0.75 mm). They probably represent fragments of LBF and mollusk tests. Echinoderm plates and spines are present as fragments (3–4 %, 0.2–0.5 mm). Sub-millimetric, coralline red algae fragments occur (<5 %). Pale green glauconite frequently fills in the different tests and appears as fine clayey material which is associated to anhedral, opaque minerals (pyrite, magnetite). Individual grains of glauconite are absent from the matrix. A detrital component is noticeable and corresponds to anhedral to subanhedral, often calcified plagioclase crystals (2–8 %, 0.1–0.7 mm).

The different constituents are enclosed in a brown-green micrite which makes up to 30 % of the foraminiferal limestone. Rare nannofossils could be extracted from this matrix (see below). This LBF-rich facies is defined as a *Lepidocyclina* packstone with a biolithoclastic matrix (Fig. 8p).

Facies F4: sandy coral rudstone

Sandy coral limestones (F4) crop out on the eastern part of the island and are approximately 3 m thick (Figs. 7, 8j). This facies could not be observed in thin-section, due to its highly brittle nature. Although it contains detrital minerals, the brown, mud-sized matrix of the sandy coral rudstone appears to be more carbonate-rich when compared to the one described for the *Lepidocyclina* packstone. The detrital fraction is composed of sand-sized feldspars and opaque minerals. Millimeter-sized bivalve shells are common in the matrix. The proximal part of the bed is progressively enriched in mm- to cm-sized, hermatypic coral debris (rubble), from the bottom to the top. In the distal part of the bed (to the SE), the coral communities are preserved in original growth position and appear as dm-sized, encrusting to sometimes domal, moderately packed specimens enclosed in a soft wackestone matrix.

Facies F5: rhodolith-branched coral rubble rudstone

The rhodolith-branched coral rubble rudstone (F5) represents a 1.5-m-thick deposit, which is discontinuously exposed below the main nodular coral facies and overlies the sandy coral rudstone (Figs. 7, 8c, e–h). It is mainly made of mm- to cm-sized, closely packed rhodoliths (40–70 %). The forms are concentric, spheroidal to ellipsoidal to sometimes columnar rhodoliths, sometimes covered by encrusting Foraminifera and embedded in a muddy matrix (Fig. 8g, h). Reworked debris of branched corals (rubble) are present in the upper part of the rudstone in 0.5-m-thick lenses (Fig. 8c). Coral debris appear like intermingled tubes (60–70 % of the bed volume) with lengths up to 5 cm and correspond to dismembered branches of an originally arborescent framework (Fig. 8e). Coherent pieces of the framework are also observed (Fig. 8f). Although the coral debris are sometimes encrusted by red algae, a pervasive algal binding as well as rhodoliths are absent from the rubble. The latter is bound by diagenetic cements. The rhodolith-coral rubble facies is considered as a rudstone, as the rhodoliths and the rubble do not build a rigid framework and were possibly locally transported/reworked.

The microscopic observation of the rhodolitic part of the rudstone facies allows for a more detailed description of the red algae. The mm- to cm-sized rhodoliths display a thick concentric structure developed around a nucleus, with crusts of Melobesioid crustose red algae (Fig. 8i). The monospecific, millimetric algal crusts show the presence of conceptacles, encrusting Foraminifera and sometimes trapped matrix. Rhodoliths smaller than 1 cm in diameter (elongated forms) adopt the shape of the nucleus, while the ellipsoidal to spheroidal, larger forms display warty crusts that do not usually outline the nucleus shape. For the smaller forms, the crust thickness is roughly equivalent to the nucleus radius. When it exists, the nucleus corresponds mainly to mm-sized debris of corals and in minor proportions to matrix intraclasts and unrecognizable calcitic clasts. This rhodolith-rich facies shows in places a nodular fabric which is related to a pressure solution process. Effects of this process are partly localized on the rims of the rhodoliths, which display ferruginous dissolution seams at the boundaries with a microspar matrix (sensu Folk 1965). The latter also develops dissolution seams highlighted by ferruginous zones.

Other bioclasts (15 %) are present in the rudstone matrix. Millimeter-sized gastropod shells commonly occur in longitudinal and transverse sections. Smaller benthic Foraminifera are scarce (0.25–1 mm). Altered fragments of echinoderm plates and spines display sizes from 0.2 to 2 mm. Finally, the least common skeletal grains correspond to mm-sized fragments of Udoteacean green algae and sub-millimetric fragments of bivalves. The detrital component

is almost absent and consists of anhedral to subanhedral plagioclase crystals (0.25–0.75 mm).

Facies F6: nodular coral framestone

The coral framestone facies (F6) crops out all over the Isla Juanilla in nodular beds which take the shape of prograding clinoforms in the central area of the island (units U2 to U5; Figs. 7, 8c). The maximum exposed thickness of this facies does not exceed 20 m, but may be thicker in the central part of the island (see transect D-D', Fig. 7). The coral nodular framestones display a beige fresh surface and are primarily made of massive corals associated to red algae. The nodular aspect of the decimetric beds (0.2–0.5 m) is due to the abundant presence of coral colonies (40–65 %) and is particularly visible on the southwestern part of the island. The bedding is not developed in the first 3 m of the facies, which appear as a structureless, massive lithology. The corals show recrystallized, sometimes well-preserved, spheroid to domal shaped colonies with decimetric sizes (up to 0.8 m). We have distinguished a few species and genera in the field (Fig. 12), which are listed below. Millimeter-sized red algae clasts are commonly observed in the coral framestone matrix.

Microscopically, the corals are observed as mm- to cm-sized corralite frameworks, as well as reworked debris (Fig. 8d). The corals are set in a dark grey, poorly sorted matrix showing characteristics of a packstone, which also fills in the coral septas. The original mineralogical composition of the coral skeletons disappeared since they display drusy and coarse sparite in the studied sections. Melobesioid and Sporolithacean coralline red algae are present in the micritic matrix as well-rounded clasts (0.15–10 mm, 15 %; up to 40 % in some grainstones). Other bioclastic elements (15 %) are present in the nodular coral framestone. Millimeter-sized gastropod shells commonly occur in longitudinal and transverse sections. Smaller benthic Foraminifera (0.25–1 mm) and altered fragments of echinoderm plates and spines (0.25–2 mm) are generally scarce. The least common bioclasts correspond to mm-sized fragments of Udoteacean green algae and sub-millimetric bivalve fragments. The detrital component is almost unnoticeable and consists of anhedral to subanhedral crystals of plagioclase (0.2–0.4 mm). The coral-rich facies can be considered as a coral framestone with a bioclastic packstone matrix, as it appears as a three-dimensional in situ rigid framework which supports the rock. This facies displays the most diverse coral fauna of the Juanilla Fm.

Facies F7: Lepidocyclina-encrusting coral bindstone

This 5-m-thick nodular facies overlies the coral framestone facies and crops out in the overturned limb of the

recumbent fold (slump) located in the northwestern Isla Juanilla (Fig. 7). The lithology consists mainly of cm-thick, elongated, closely packed encrusting corals (*Hydnophora* sp.) which can reach lengths up to 50 cm (Fig. 8a, b), and a few massive, decimetric corals of the genus *Caulastrea* (Fig. 12c). Some bindstone beds display cm-sized, curved *Lepidocyclina* tests (25–30 %, IJ18; Figs. 8a, b, 11g, j). The corals and the lepidocyclinid tests are commonly encrusted by coralline red algae (0.75–1 mm thick) and show evidence of bio-erosion by boring organisms. The packstone matrix of the bindstone contains other bioclasts (20–25 %, 0.15–1 mm) which correspond to smaller benthic Foraminifera and poorly sorted fragments of crustose red algae, echinoid spines and corals. The bioclasts are embedded in a microspar matrix (crystals 10–40 µm in size; Fig. 8b).

Age of the Juanilla Formation

Larger Benthic Foraminifera The beds rich in LBF (facies F3, sample IJ5; Figs. 7, 8k, 11) yielded up to 90 % of *Lepidocyclina* sp. consisting commonly of very thin, up to 6 cm in diameter, microspheric forms. Some of these have undulations like the forms described by Vaughan (1919) from the Oligocene of Trinidad, such as *Lepidocyclina undulata* Cushman. Among the macrospheric forms, we distinguished many nephrolepidine and eulepidine embryon types. The sample IJ5 contains *Lepidocyclina* (*Nephrolepidina*) *vaughani* Cushman, *Lepidocyclina foresti* Vaughan, *Lepidocyclina undosa* Cushman, *Lepidocyclina* (*Eulepidina*) *favosa* Cushman, *Lepidocyclina canellei* Lemoine and Douvillé and *Miolepidocyclina* cf. *panamensis* in few oblique sections. We also determined *Miogypsinoides* sp., in which we could not count the number of periembryonic chambers by lack of equatorial sections. Hence, we could not distinguish between *Miogypsinoides butterlinus* and *Miogypsinoides complanatus*. Several of these taxa indicate a late Oligocene age. This sample also contains questionable *Helicosteginoides* sp., identified under cathodoluminescence by its nepionic stage, and considered to be restricted to the Eocene. However, this form shows corrosion that suggests reworking. Forms of the same family, such as *Helicosteginoides soldadensis*, *Helicocyclina paucispira*, *Helicosteginoides intermedius* have been found in the Cipero Formation of Trinidad known from the Oligocene (Kugler 2001). These forms were also considered as reworked by Caudri (1975) because they are until now only known from the Eocene of the Caribbean.

The sample IJ18 (facies F7; Figs. 7, 8a, 11) contains *Lepidocyclina* (*Eulepidina*) *favosa* Cushman and *Lepidocyclina canellei* Lemoine and Douvillé. This association of LBF indicates also a late Oligocene age (Cole 1952, 1961; Butterlin 1962; Caudri 1996).

Hermatypic corals Several sites on the east side and at the NW-tip of Juanilla Island have yielded well-preserved hermatypic coral species (Fig. 12). *Siderastrea conferta* Duncan (Fig. 12a, b), was described from the upper Oligocene Antigua Fm. of Antigua and Barbuda (Lesser Antilles; Vaughan 1919). This species has also been described from the lower Oligocene of Jamaica (Stemann 2004). This seems to be the oldest occurrence. *Antiguastrea cellulosa* Duncan (Fig. 12d, e) has been also described form the upper Oligocene Antigua Fm. (Frost and Weiss 1979). It is also present in the lower Oligocene of Jamaica and Hispaniola (Vaughan et al. 1921; Stemann 2004). We found at least two species of *Hydnophora* (Fig. 12g–i). Today, this genus is restricted to the Indian Ocean and Australia. It is so far unknown from the American margin. It ranges, however, from the Mesozoic to Recent. In particular, it has been described form the Eocene and Oligocene of the Caribbean. The genera *Caulastrea* (Fig. 12c) and *Diploastrea* are typical of the modern Indopacific realm, but were present in the Caribbean until the Pleistocene. In summary, the two identified coral species confirm a (possibly late) Oligocene age of the Juanilla Fm.

Nannofossils We have extracted scarce calcareous nannofossils from the mud-sized matrix of the *Lepidocyclina* packstone (F3). Several species were determined (written communication: Simonetta Monechi, University of Florence). *Discoaster tanii* and *D. deflandrei* range through the Eocene–Oligocene, whereas *D. lenticularis*, *D. sublodoensis* and *D. barbadiensis* seem to be reworked from the underlying Eocene formations. Unfortunately, no nannofossils characteristic of the Oligocene could be found, perhaps due to the paralic conditions at that time.

Reef growth

General features

Tectonic uplift that was responsible for the erosion of much of the underlying Junquillal Fm. gave way to moderate subsidence, creating accommodation space for reef growth during a time of an overall constant eustatic sea-level (Haq et al. 1987; Haq and Al-Qahtani 2005; Miller et al. 2005). A 4th–5th order glacio-eustatic sea-level rise, coinciding with the Milankovitch frequency band (Tucker 1993; Einsele 2000), could also have triggered reef growth, but its preservation implies at least moderate subsidence.

The unconformable onset of photozoan carbonate sedimentation on the substantially eroded uplifted high (facies F1–F2) could not be clearly observed due to the lack of outcrops (Fig. 7). It occurred after a time of erosion and/or non-deposition encompassing at least the early Oligocene. However, the onset of reef building in the youngest coral reef unit (U6) has been described with more detail and is

noticeable in the shallowing-upward transition from the facies F3–F4–F5 to the facies F6 (Figs. 7, 8). As suggested in the U1 stratigraphic column (Fig. 7c), we admit that the shift from the uplifted siliciclastic shelf deposits (F2, Junquillal Fm.) to the reef facies (F6) possibly occurred trough the deposition of the facies F3–F4–F5. It is not clear whether the substrate underlying the coral reef facies F6 is similar for the different units (U1–U6). The facies F3–F4 represent platform sediments that deposited prior to the reef core unit (U1), in a rather low-energy, siliciclastic-influenced environment. Subsequently, the coral reef prograded and aggraded on these platform deposits, with the deposition of the units U1 to U6. The unit U6 possibly represents the evidence for such a process (Figs. 7, 8c, d).

The period over which the Isla Juanilla Coral Reef grew cannot be estimated with the dated fossils (low time resolution). Although the exposure of the Juanilla Fm. may be incomplete, the Isla Juanilla Coral Reef presents a size which is comparable to some Holocene fringing reefs. Holocene coral reefs of similar sizes commonly constructed most of their framework within periods shorter than 8000 years (Kennedy and Woodroffe 2002; Montaggioni 2005). In the Caribbean realm, Holocene reefs grew at mean rates of 6 m/1000 years, which is comparable to growth rates of pre-Holocene reefs exposed around the world (Dullo 2005).

Pre-reef stage 1: calm water, offshore conditions (facies F3: Lepidocyclina packstone)

The first phase of carbonate platform development is marked by the colonization of the uplifted substrate by an oligophotic fauna (LBF and solitary corals). The facies F3 is also characterized by the occurrence of solitary corals and abundant presence of mud (Fig. 8o), which indicates low light/low energy conditions. The accumulation of well-preserved, bed-parallel *Lepidocyclina* tests (Fig. 8k) is indicative of a low-energy environment of deposition. Moreover, the well-preserved, delicate tests have apparently not suffered much transport and have accumulated in situ, forming a 7-m-thick bed. This is also the case for the other large bioclasts, which have not experienced any significant breakage. The poorly sorted fragments of mollusks and lepidocyclinids probably originate from the in situ destruction by predators.

This environment was under the influence of a slight terrigenous input, highlighted by the presence of angular, sand-sized plagioclase grains and a clay-rich micritic matrix. Coral reef-derived bioclasts are absent, implying that there was no connection with a reefal environment. Glauconite growth in the porosity of bioclasts in association with pyrite is thought to have been favored by the presence of organic matter, acting as a reducing micro-environment

(Huggett and Gale 1997; Kelly and Webb 1999; Chafetz and Reid 2000; Baldermann et al. 2012). The pale blue-green fresh surface of the rock suggests fine-grained impregnation of the matrix by glauconite, although it is not clearly visible in thin-section. The depositional paleodepth of the *Lepidocyclina* facies is certainly restricted to the photic zone (Frost and Langenheim 1974; Sartorio and Venturini 1988; Hottinger 1997), as the lepidocyclinids have probably hosted photosymbionts in their tests (Chapronière 1975; Brasier 1995). Large lepidocyclinids (very low thickness/diameter ratios) could have proliferated in quiet, low-light environments down to the lower photic zone (Hallock and Glenn 1986; Hottinger 1997). Behforouzi and Safari (2011) describe a clear morphologic change of the *Lepidocyclina* tests, with increasing depth and decreasing light intensity and hydrodynamic energy. Very thin tests are characteristic of low light/low energy conditions. This is in accordance with the presence of numerous solitary corals, which can settle on soft substrates in turbid, reduced light conditions (Schuster and Wielandt 1999). Whereas clayey sedimentation and turbidity prevented the settlement of larger, hermatypic corals (Sanders and Baron-Szabo 2005). Such conditions also explain the occurrence of irregular, infaunal echinoids. These different elements suggest that the *Lepidocyclina* facies was deposited in a low-energy, probably rather mesotrophic environment which was connected to a source of suspended detrital material (Seyrafian et al. 2011). The low-energy conditions allowed also the deposition of planktonic organisms (coccoliths) brought in by open-marine circulation. Nevertheless, it remains difficult to estimate the water depth of deposition, as the photic zone could have been reduced due to detrital input and turbidity.

In the literature, there is a long debate on the origin of massive LBF accumulations. Hypotheses of in situ growth and accumulation are opposed to accumulation due to lateral transport by bottom currents and wave action. A nice overview of the early work is given by Matteucci and Pignatti (1989) showing Arni's (1963) nummulite bank hypothesis as well as Aigner's (1982, 1985) model of massive almost monospecific nummulite accumulations, considered as an interaction of biological and hydrodynamical processes. Based on the relative abundances of A- versus B-forms, Aigner (1985) distinguished: (1) thanatocoenoses and in situ winnowing (A ≫ B); (2) selectively winnowed assemblages enriched in B-forms (A > B); (3) residual assemblages (B only); (4) allochthonous assemblages (A only) formed by hydrodynamic transport and settling (e.g., turbidites).

Our facies F3 seems to be relatively enriched in B-forms at the outcrop scale (Fig. 8), but A-forms are well represented in thin-sections. From this point of view the assemblages can be considered as para-autochthonous.

More recently, Briguglio and Hohenegger (2009, 2011) and Seddighi et al. (2015) combined laboratory settling experiments, observations in modern coastal-offshore environments of Okinawa (Japan) and modeled hydrodynamic conditions to understand the relationship between LBF shape and the hydrodynamic densities and conditions in the specific habitat. Although these studies mainly dealt with nummulitids, they may give some hints to the interpretation of the *Lepidocyclina* beds (facies F3) of Juanilla Island. The large, very flat lepidocyclinids have a relatively low density, a low shape entropy (Hofmann 1994; Briguglio and Hohenegger 2009), and hence a low settling velocity. Once settled, they tend to be more easily resuspended by wave action and transported by lateral currents than ellipsoidal forms. The conclusion is that facies F3 was formed in calm waters, essentially beneath the storm weather wave base. This is confirmed by few broken or abraded forms and the abundance of clays in the matrix. On the other hand, the large *Lepidocyclina* tests, once settled on a cohesive sediment, are less prone to resuspension (Hjulström diagram; Hjulström 1935). Therefore, water depths derived from modern observations in sandy, carbonate environments cannot be directly applied to the *Lepidocyclina* beds of Juanilla.

Pre-reef stage 2: shallowing conditions (facies F4: sandy coral rudstone)

Although rather mesotrophic conditions still prevailed at this stage of platform sedimentation, the deposition of the sandy coral rudstone (facies F4; Fig. 7) represents the first occurrence of hermatypic coral communities. Although the presence of mud was reduced in comparison with facies F3, the corals probably grew on a pavement of LBF and other bioclasts from the previous, turbid, poorly illuminated environment. This facies change was the result of a shallowing of the platform floor in response to a 4th–5th order eustatic sea-level drop and the accumulation of LBF-rich sediments. The shallowing resulted in an increase of water energy and evacuation of mud towards offshore settings, thus increasing light penetration.

The facies F4 proximal deposits consist of coral rubble, whereas the distal ones display low-diversity coral assemblages in growth position (Fig. 8j). This facies distribution suggests that initial coral growth may have been preferentially located in the deeper, less agitated parts of the uplifted high. The shallowest areas were prone to constant wave action and periodical storms. These conditions could have prevented the permanent settlement of corals. The laminar morphology of the corals in the distal deposits suggests a rather low-energy environment with low turbidity and limited sediment accumulation. In these reduced light conditions, the corals produced thin, encrusting shapes to

maximize their light-capturing surface (Wilson and Lokier 2002). However, the low light conditions hindered the construction of a reef framework. The corals remained as individual bioconstructions, separated by episodically deposited, mud-rich sediments. It is not excluded that some of the corals switched from autotrophic to heterotrophic modes of nutrition during episodic turbid pulses (Anthony and Fabricius 2000).

Pre-reef stage 3: shallow conditions (facies F5: rhodolith-branched coral rubble rudstone)

The subsequent deposition of mud-poor, rubble- and rhodolith-rich sediments attest for more oligotrophic conditions. The increasing wave energy permitted the circulation of clear waters that lasted for most of the following reef growth. Moderate- to high-energy, euphotic conditions are recorded by spheroidal to ellipsoidal, concentric rhodoliths that developed thick, homogeneous crusts (Braga and Martin 1988; Bosence 1991; Fig. 8g–i). Coral rubble was produced by the action of waves and storms in water depths shallower than 20 m (Rasser and Riegl 2002). The rubble and the rhodoliths originated in biodetrital crests formed around the shallowest edge of the uplifted high.

Coral rubble (facies F5) is composed of small, almost monospecific branching forms that colonized the platform floor (=facies F4), shortly prior to the growth of the Isla Juanilla Coral Reef (Figs. 7, 8). Initially, the relatively soft platform floor favored the establishment of low-diversity, branching forms due to their wide physiological tolerances, including the ability to proliferate by fragmentation and resilience to taphonomic destruction (Wood 2011). Subsequently, the rubble deposits acted as a hard, stable substrate for the larval recruitment of other, more diverse coral species (large coral heads, facies F6; Figs. 7, 8). These species rapidly supplanted the delicate, pioneer forms, initiating the building of the reef framework.

Reef stage 1 (=unit U1): catch-up phase (facies F6–F7: coral framestone and bindstone)

The first phase of reef framework accretion (unit U1) occurred vertically, as accommodation space was still available between the platform floor and the sea surface. The available space was filled with reef facies F6 and F7 (Figs. 7, 8).

The framestone facies (F6) consists of massive, domal to tabular morphologies which typically proliferated in moderate- to high-energy, oligotrophic conditions (James 1983). They colonized the shallowest and most agitated parts of the carbonate platform, previously occupied by rubble- and rhodolith-rich crests. The close co-occurrence of photosynthetic corals in growth position and coralline
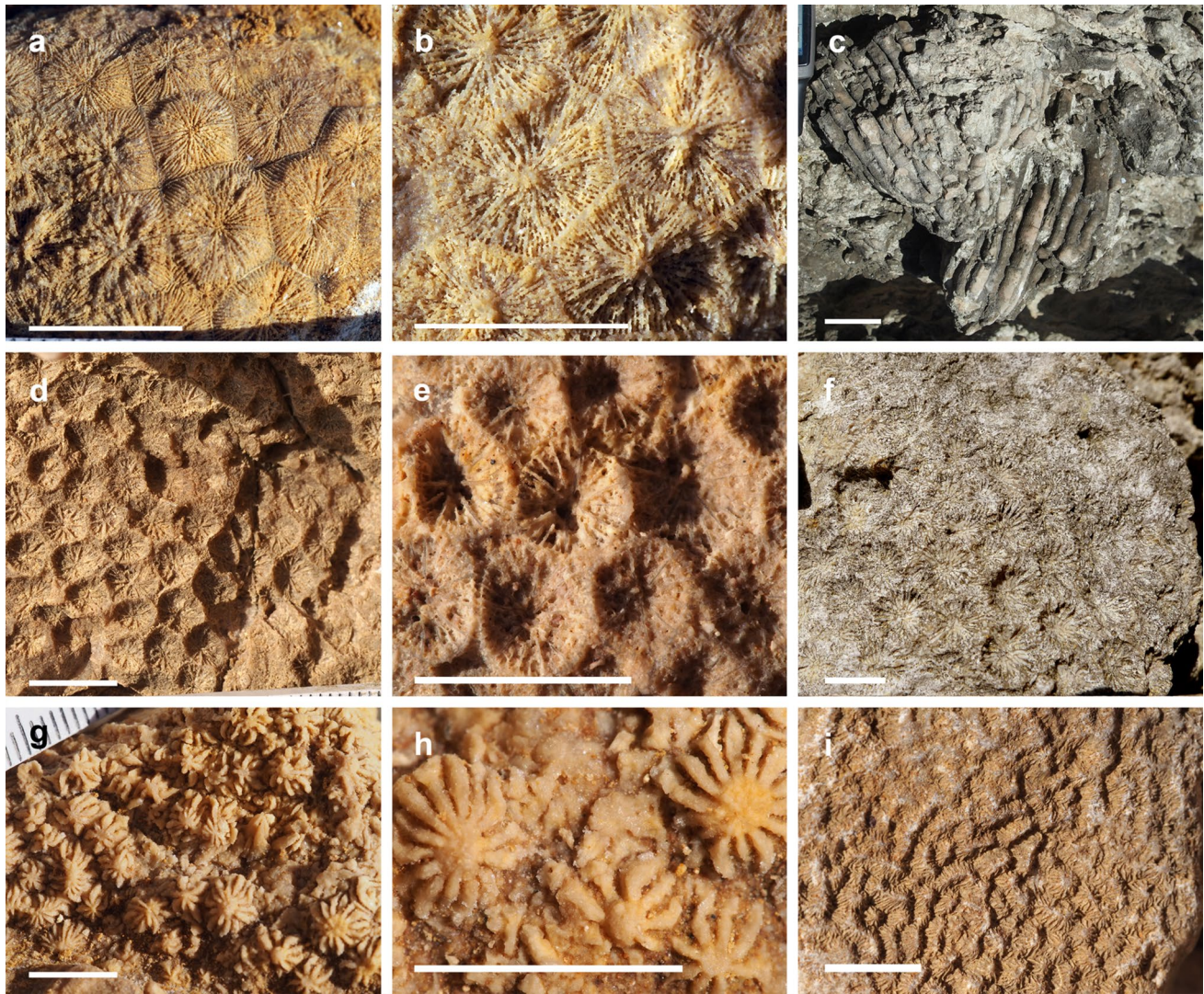
Fig. 12 Hermatypic corals of the Juanilla Formation. *Scale bar* is 1 cm for all figures except for **c** 3 cm. **a, b** *Siderastrea conferta* Duncan. **c** *Caulastrea* sp. **d, e** *Antiguastrea cellulosa* Duncan, very simi-lar to holotype from the upper Oligocene Antigua Fm. (Antigua and Barbuda). **f** *Diploastrea* sp. **g, h** *Hydnophora* sp. A. **i** *Hydnophora* sp. B

algae, as observed in the nodular coral framestone (facies F6), has been reported as a typical reef-building association in Cenozoic, tropical to subtropical environments (Heckel 1974; James 1983; Fagerstrom 1988). These communities generally colonized hard substrates in the agitated, shallow photic zones, where the input of nutrients and terrigenous sediments was low (Muscatine and Porter 1977; Hallock and Schlager 1986; Brasier 1995; Wood 1999).

The deposition of the bindstone facies (F7) occurred on a reef crest, forming a reef top. The resulting intense wave energy is reflected in the coral morphology/size (mainly cm-thick encrusting forms; see Montaggioni 2005 for Holocene examples; see Fravega et al. 1994 for an Oligo-cene example) and diversity (only 2 genera). The encrust-ing, slow-growing coral habits evidence an adaptation

to frequent and intense wave energies. The decline of the coral diversity and the disappearance of domal morpholo-gies may have occurred in a very short period (<10 years; Wood 1999). Moreover, the physical disturbances led to the subsistence of only a few other resilient species. These include crustose red algae, borer communities, and LBF occurring in few niches. Except for red algae, these organ-isms are absent from the reef facies F6, which accumulated in less agitated conditions.

During the reef building initiation, the available accom-modation space may have been at most 20 m. This is deduced from the unit U1 thickness (~18 m), which upper-most 5 m (facies F7) deposited once the reef reached the sea surface. Similarly, in Holocene fringing reefs, the abil-ity of corals to construct a vertically accreting framework is
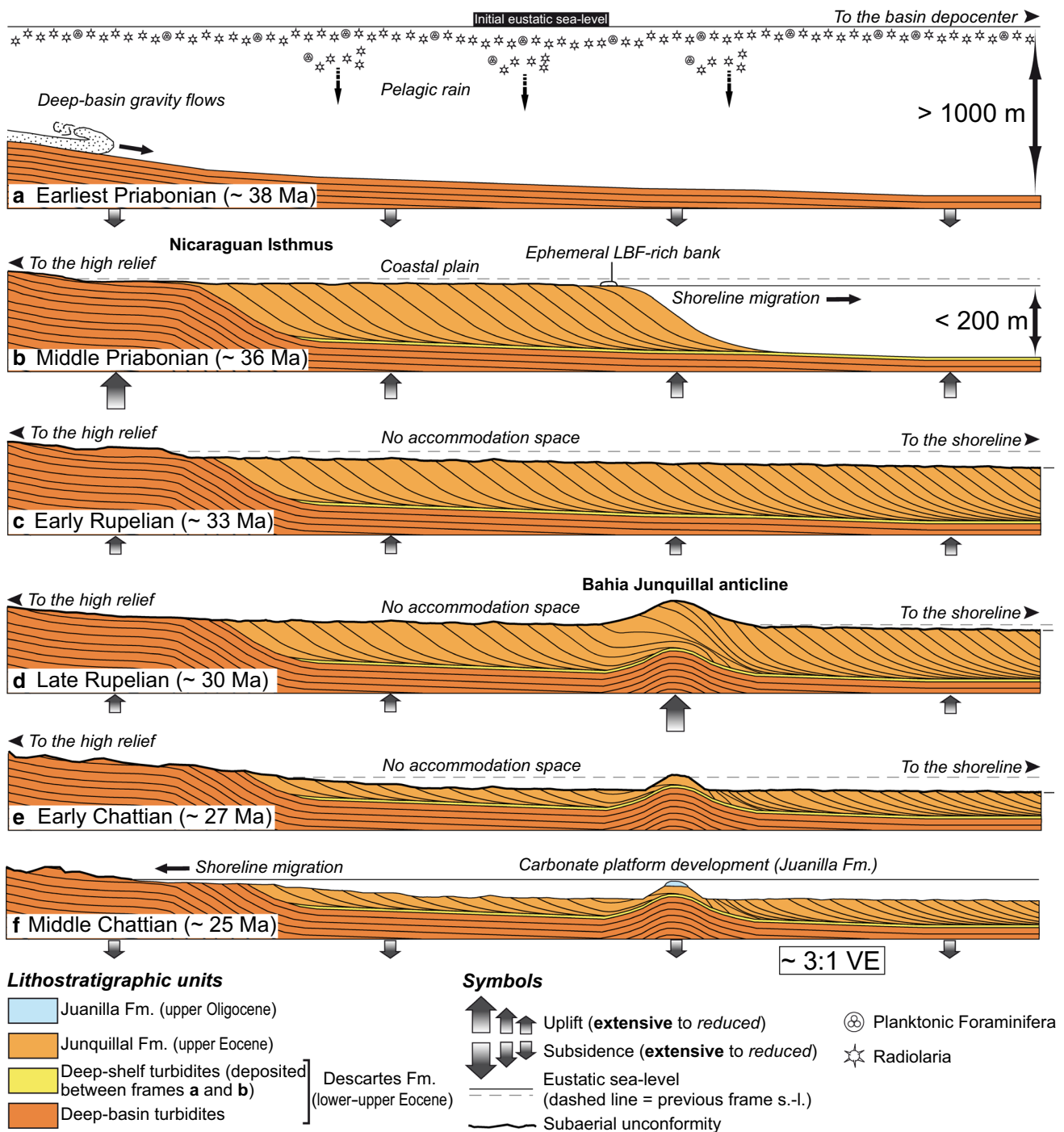
Fig. 13 Schematic model depicting the upper Eocene–Oligocene tectono-sedimentary evolution of the southeastern Sandino Forearc Basin (3:1 vertical exaggeration). See "Discussion" for more details. **a** Interplay between turbiditic and pelagic sedimentation in a deep-basin environment (Descartes Fm.). The basin depocenter is located a few kilometers seaward. **b** Differential uplift of the forearc basin leading to emergence of the Nicaraguan Isthmus. The deep-shelf turbidites correspond to the facies F1 in Fig. 7. Seaward progradation of shallow-shelf units (Junquillal Fm.) under a slightly falling sea- level regime. **c** The conjunction of sea-level fall (55 m) and ongoing uplift causes the subaerial erosion of the Junquillal Fm. The locus of shelf sedimentation migrated seawards (not visible in the frame). **d** Localized folding of the sedimentary pile, thus creating the Bahia Junquillal anticline. **e** Deep erosion of the Junquillal Fm. due to the mid-Oligocene sea-level fall (~55 m). Tectonic quiescence. **f** The sub- sidence of the shelf provokes a relative sea-level rise (transgression). The newly created accommodation space favorizes the establishment of a carbonate platform (Juanilla Fm.) on the uplifted tectonic high

limited to the uppermost 20 m of the water column, where favorable light saturations occur (Bosscher and Schlager 1992; Montaggioni 2005).

Post-depositional deformation of the unit U1

The unit U1 is comprised in a recumbent fold overturned towards the SW (profiles A–A', B–B'; Fig. 7b). On the northwestern coast, the unit U1 appears as a 300-m-long dip slope with SW-directed dips varying from 65° to 45° (profile D–D'; Fig. 7b). The recumbent fold affects the reef framework with more than m-sized coral colonies. However, no brittle fracturation can be observed in the limestone. We conclude that this deformation occurred prior to lithification of the reefal matrix and may represent post-depositional, gravitational slumping of the unit U1 (facies F6–F7). The fact that the underlying facies (F1–F5) are less consolidated and rich in clays may have favored slumping in the seismically active forearc area. The units U2–U6 show no evidence of deformation, which indicates that they deposited after the slumping event. Actually, a major unconformity separates the unit U1 from the prograding units U2–U3 (profile D–D'; Fig. 7b). The steep dips (~60°) of the unit U2 reflect the topography inherited from the slumped unit U1. Further to the SSE, the dips of the units U3–U6 become flatter, as these units deposited farther from the slumped unit.

Reef stage 2 (=units U2–U5): progradational phase (facies F6: coral framestone)

Due to limited accommodation space, the reef started to accrete laterally. This progradational phase is recorded in the units U2–U5. These steeply inclined, prograding units (profile D–D'; Fig. 7b) formed a reef front which progressively advanced towards the SE, over a distance of 150 m. The wave-influenced, open marine environment was favorable to the further establishment of coral head communities. The lateral accretion was facilitated by: (1) a relatively flat topography which provided a constant accommodation space; (2) cemented rubble and rhodoliths-rich deposits (facies F5; Fig. 7) which provided a hard substrate for the advancing reef front.

Reef stage 3 (=unit U6): keep-up phase (facies F6: coral framestone)

The last phase of the reef development is recorded in the unit U6 (Fig. 7). The unit U6 consists of flat-lying framestone beds (facies F6). These beds aggraded over a fore-reef facies (F5) made of rubble and rhodoliths (Fig. 7c) and progressively onlapped the steeply inclined reef front of the unit U5 (profile D–D'; Fig. 7b). The unit U6 evidenced

the end of lateral reef accretion, following an increase in accommodation space. The coral communities tended to vertical accumulation, in attempt to match the relative sea-level rise. The latter possibly resulted from tectonic subsidence or 4th–5th order eustatic sea-level rise. Owing to optimal growing rates, the unit U6 coral communities successfully tracked the relative sea-level rise, which is deduced from: (1) the facies homogeneity of the unit U6, indicating an immediate adaptation of coral communities to the changing conditions; (2) the facies similarity (F6) between the aggrading unit U6 and the prograding units U2–U5, previously deposited at constant sea level.

Discussion

The shallowing-upward trend in the southern Sandino Forearc Basin: the role of tectonic uplift and eustatic sea-level changes

Pre-Priabonian

Prior to the late Eocene shallowing-upward trend, the SFB deposits accumulated in deep-sea settings during a period of 30 m.y. (Figs. 3, 13a). During this time, the basin development was primarily dependent on subsidence and volcanic arc activity supplying turbidites. Around the Paleocene–Eocene boundary (Buenavista Fm.), the temporary interruption of arc-derived turbidite activity may be related to a transgression (sea-level rise; Haq and Al-Qahtani 2005; Miller et al. 2005) in combination with a short-lived, cessation of arc activity, related to subduction tectonics.

Priabonian

The late Eocene epoch is characterized by a shallowing-upward succession of depositional units of the SFB as a result of tectonic uplift of the nascent Nicaraguan Isthmus (Figs. 1, 2, 13b). This forearc segment underwent a Priabonian uplift event that provoked the abrupt end of deep-water facies deposition (Descartes Fm.) and onset of coarse-grained, shelf detrital sedimentation (Junquillal Fm.). Due to limited accommodation space, the Junquillal Fm. deposits prograded seaward from the uplifted Nicaraguan Isthmus towards the present-day Punta Descartes area and downlapped over the Descartes Fm. (Fig. 13b). The transition from basinal to shelf facies happened rapidly (<2 m.y.) and is easily recognizable in the field, even if no angular unconformity accompanied this event (Fig. 5g). Actually, a major upper Eocene unconformity exists in the Nicaraguan part of the basin (treated in a separate paper). The absence of a major angular unconformity in the Costa

Rican part may be explained by a distant tilt axis resulting in uplift without important rotation.

The detailed study of the tectonic events that caused the upper Eocene–lower Oligocene shallowing-upward of the SFB is the scope of a separate paper. However, here are summarized the key points which led us to consider that the shallowing-upward trend was primarily controlled by tectonic uplift;

1. In the southeastern part of the SFB (Nicaragua), major unconformities exist between Eocene turbidites (Brito Fm.) and upper Eocene tempestites (new formation to be defined);
2. The SFB depocenter exhibits impressive, along-basin thickness variations. The southeasternmost part of the SFB consists of a 5 to 6-km-thick sedimentary pile (seismic profile NIC-20, Berhorst 2006; Funk et al. 2009; this study; Fig. 2b). The depocenter thickness increases constantly towards the NW and reaches 16 km in the northwesternmost part of the depocenter (250 km to the NW; seismic profile NIC-100; McIntosh et al. 2007). Interestingly, the pre-upper Eocene sequences present uniform facies successions and a constant, along-basin thickness of 5–6 km. On the other hand, the thickness of post-Eocene sequences increases towards the NW (<0.1 km in SE-most SFB to 10 km in the NW-most SFB), with changing depositional paleoenvironments.

We conclude here that these along-basin thickness and facies variations reflect the effects of an upper Eocene, differential uplift of the SFB. The southeastern SFB was affected by the strongest uplift. This uplift possibly affected the Tempisque Forearc Basin (SFB southern equivalent, NW Costa Rica) and may explain the absence of post-Eocene forearc deposits in this area (Denyer and Alvarado 2007). The uplift markedly limited further development of the southeasternmost SFB. Here, sedimentation probably stopped during the late Oligocene, after a period dominated by erosion and/or non-deposition (see below). At the same time, the central and northwestern SFB experienced much slower uplift rates. In consequence, the shallowing-upward trend is more progressive. In these parts, the Eocene Brito Fm. turbidites are conformably overlain by km-thick, deep-shelf carbonate-detrital sequences of the lower Masachapa Fm. (lower Oligocene; Elming et al. 1998). Later, shoreface conditions were reached during the late Oligocene, which is ~5 to 7 m.y. later than in the southeasternmost SFB. These depositional environments suggest a diachronous, along-basin shallowing-upward trend supporting a differential uplift of the SFB. In contrast with the southeastern SFB, shelf sedimentation continued in the central and northwestern SFB until the middle Miocene.

An eustatic sea-level fall (<50 m for the Priabonian; Haq and Al-Qahtani 2005; Miller et al. 2005) could have contributed to the observed facies changes by a decrease in accommodation space and filling-up of the basin. However, the eustatic sea-level drop alone does not explain the Priabonian, rapid shift from several hundreds of meters deep, turbiditic to near-shore environments and the important post-Eocene, along-basin facies and thickness variations.

Rupelian

The early Oligocene corresponds to a period of global sea-level fall which was related to the formation of major Southern Hemisphere ice sheets (Miller et al. 2005). A sea-level fall of ~55 m occurred at the Eocene–Oligocene boundary and enhanced forced regression in the southeastern SFB. The sea-level fall led to the erosion of the upper Eocene tempestites in a coastal setting (Junquillal Fm.; Fig. 13c). The eroded proximal shelf sediments contributed to the regressive-forced sedimentation which was possibly localized in the distal shelf.

Compressional tectonics were still active and caused the folding of the central and southeastern SFB. The SFB exhibits folds that have been imaged by seismic profiles in its southeastern and central segments, and include the Corvina and Argonaut anticlines (Ranero et al. 2000; Berhorst 2006; Sallarès et al. 2013). The origin of these localized structures remains debated. They formed either in reaction to transpressional forces (arc-parallel strike-slip faults; Ranero et al. 2000) or by a mechanism of out-of-syncline thrusting (orthogonal compression in an extensional context) which accompanied the uplift of the Nicaraguan Isthmus (Funk et al. 2009). Indeed, the co-occurrence of these regimes is common in active margins (Bally et al. 2012). In any case, the folds grew during the deposition of the lower Masachapa Fm. (lower Oligocene; Ranero et al. 2000) and caused an uplift of the forearc lithologies comprised between 0.4 and 1.7 km. In the studied area, these compressional and/or transpressional forces led to the local folding and uplift of the forearc formations, thus forming the Bahia Junquillal anticline (Figs. 2, 13d; formed prior to the Bahia Junquillal synform). The folding/uplift event initiated the local, subaerial erosion of the Junquillal Fm. which would continue until the early Chattian. The conjunction of eustatic sea-level fall and tectonic uplift caused a general erosion/non-deposition of sediments in the former proximal shelf.

Chattian

The global sea-level stabilized during the Chattian, after an important fall at the Rupelian–Chattian boundary (160 m after Haq et al. 1987; 100 m after Haq and Al-Qahtani

2005; 55 m after Miller et al. 2005). The sea-level fall caused further erosion of the Junquillal Fm. tempestites. Due to the conjunction of the Rupelian uplift (see above) and continuous sea-level fall, the tempestites comprised in the Bahia Junquillal anticline were almost completely eroded to <10 m on the Isla Juanilla (Figs. 7, 13e). In comparison, the tempestites located off the Bahia Junquillal anticline show much thicker exposures (apparent thickness up to 2000 m; Fig. 2a). This differential erosion of the Junquillal Fm. indicates that the Bahia Junquillal anticline was an uplifted tectonic high during the Oligocene and became the substratum on which the Juanilla Fm. deposited (Fig. 13f). The ephemeral development of the carbonate platform in a siliciclastic-poor environment was facilitated by an overall constant sea-level and relaxation of the tectonic stress. These factors and perhaps 4th–5th order eustatic sea-level changes provided the essential conditions for a short-lived carbonate shoal development: (1) subsidence produced accommodation space, which was extremely reduced during most of the Oligocene; (2) the locus of detrital sedimentation was displaced towards more proximal settings due to relative sea-level rise. The decreasing detrital input facilitated the establishment of oligotrophic conditions suitable for reef growth.

The Juanilla Fm. experienced syn-reef deformation, evidenced by the recumbent fold affecting part of the Isla Juanilla Coral Reef (unit U1; Fig. 7a, b). Post-depositional seismic activity may have triggered gravitational slumping of the unit U1. We favor this interpretation because: (1) only large scale, open folds (e.g., Bahia Junquillal synform; Fig. 2) of the late Neogene–Quaternary tectonic phase are exposed (Weinberg 1992); (2) the slumping event deformed only the unit U1 of the Juanilla Fm. (Fig. 7b), and not the underlying lithologies (facies F1–F5) and the units U2–U6.

Occurrences of Oligocene shallow-water carbonates in Costa Rica

In Costa Rica, the few exposures of Oligocene shallow-water carbonates have been regrouped as the Punta Pelada Fm., defined by Sprechmann et al. (1994). However, the Punta Pelada Fm. has to be regarded as an approximately Oligocene chronozone and not as a formation in the sense of Hedberg (1976), because it includes, as defined by different authors (see in Aguilar and Cortés 2001), exposures representing two distinct sedimentary basins, with very different sedimentologic and paleogeographic settings: (1) in the Punta Pelada-Punta Nosara area (Nicoya Peninsula western shore), the sections exhibit tens of meters of upper Oligocene, sandy bioclastic limestones, made of LBF, bivalve fragments and echinoderms, displaying high-angle cross-stratification. These outcrops were interpreted as shallow carbonate-detrital banks in which

submarine dunes formed above the fair-weather wave base, in an outer forearc-high setting (Baumgartner et al. 1984; Baumgartner-Mora et al. 2008); (2) in the Turrialba area (Cartago Province, central Costa Rica), outcrops grouped with the Punta Pelada Fm. occur in quarries as 10 to 12-m-thick upper Oligocene–lower Miocene, massive or brecciated bioclastic limestones and calcarenites intercalated with volcaniclastic conglomerates and arenites (Aguilar 1999; Aguilar and Cortés 2001). The limestones are composed of abundant corals, calcareous red algae, LBF and mollusks with minor occurrences of echinoderms, crustaceans and bryozoans. Some of the limestone intervals appear as 2 to 5-m-thick, irregularly distributed, patch reefs displaying a low-diversity coral assemblage (three species representing three genera) dominated by *Antiguastrea cellulosa*. These outcrops were interpreted as patch reefs in a mesotrophic back-arc environment. The two exposures grouped as the Punta Pelada Fm. do not comprise extensive reef structures such as the upper Oligocene Isla Juanilla Coral Reef (Juanilla Fm.), which is built of a dense, three-dimensional organically constructed framework exposed over a distance of at least 700 m. In the Isla Juanilla Coral Reef, siliciclastic sediments are rare, although it developed in a siliciclastic-dominated, forearc setting. In comparison to the Isla Juanilla Coral Reef, the Punta Pelada Fm. deposits were under the constant influence of detrital input.

The shallow-water limestones attributed to the Punta Pelada Fm. and the Juanilla Fm. have in common that they unconformably overlie siliciclastic and/or hemipelagic deposits that were uplifted and eroded, resulting in places in a several-million-year hiatus between the substrate and the shallow-water carbonates (Seyfried et al. 1991; Amann 1993; Aguilar 1999; Krawinkel et al. 2000; Aguilar and Cortés 2001; Baumgartner-Mora et al. 2008). However, the uplift of the siliciclastic deposits for the three areas did not occur in the same tectonic context. The bioclastic limestones of the Punta Pelada-Punta Nosara encroached unconformably over the hemipelagic siliceous mudstones and turbidites of the Rio Ario Fm., following an uplift event in an outer high setting (Baumgartner-Mora et al. 2008). The bioclastic limestones and the patch reefs of the Turrialba area deposited unconformably over the hemipelagic mudstones and turbidites of the Senosri Fm., following an uplift event in a back-arc setting. Finally, the Juanilla Fm. developed unconformably over the amalgamated, massive tempestites of the Junquillal Fm., following an uplift event in a forearc basin setting. Although the three lithostratigraphic units may be partly contemporaneous, the Juanilla Fm. is not attributed to the Punta Pelada Fm. for the following reasons: (1) the three lithostratigraphic units did not form in the same basin; (2) there are obvious facies differences between the three carbonate units; (3) the three

lithostratigraphic units did not form in the same paleo-tectonic setting.

Occurrences of Oligocene coral reefs in the Caribbean realm

It appears that several Oligocene (to lower Miocene in some cases) coral reefs exist in the Caribbean realm, including a wide spectrum of reef morphologies and paleoenvironments (Budd 2000; Johnson et al. 2008). Lower Oligocene coral reefs are present only in Mexico (Rancho Berlin Fm.; Frost and Langenheim 1974). Upper Oligocene coral reefs have been studied in Antigua (Antigua Fm.; Weiss 1994), Puerto Rico (Juana Diaz and Lares fms.; Frost et al. 1983) and Dominican Republic (Tabera Fm.; Saunders et al. 1986). Upper Oligocene–lower Miocene coral reefs are known from Mexico (La Quinta Fm.; Frost and Langenheim 1974), Venezuela (San Luis Fm.; Díaz de Gamero 1977), Jamaica (Browns Town Fm.; Mitchell 2013) and Puerto Rico (Montebello Limestone Member, Cibao Fm.; Monroe 1980).

Concluding remarks

In the present paper, we have established the existence of two new formations cropping out in the Costa Rican part of the Sandino Forearc Basin. They correspond to the upper Eocene Junquillal Fm. and to the upper Oligocene Juanilla Fm. The Junquillal Fm. consists of tempestites and channelized boulder conglomerates that suggest proximity to a high relief shore line and hinterland. An important shallowing-upward event in the southeastern Sandino Forearc Basin is evidenced by these deposits previously attributed to the deep-water, Eocene Descartes Fm. The newly defined geological units correspond to sediments which evidenced the shallowing-upward trend of the Nicaraguan Isthmus and the subsequent folding of the neighboring Sandino Forearc Basin depocenter.

We propose that the upper Oligocene Juanilla Fm. deposited on an anticline that developed during the early Oligocene, contemporaneously to other folds observed in the offshore SFB. Prior to the carbonate platform establishment, the folded tectonic high underwent deep erosion during a period of global sea-level fall, followed by a subsidence episode during a period of 4th–5th order glacio-eustatic sea-level changes during an overall constant sea-level. Under these conditions, the uplifted and deeply eroded siliciclastic substratum facilitated the ephemeral growth of the Isla Juanilla Coral Reef in an oligotrophic, siliciclastic-poor environment.

The upper Oligocene Isla Juanilla Coral Reef represents a unique example of an extensive coral reef buildup in Central America. This reef represents a perfect example of short-lived, shallow-water carbonate shoals which formed in response to tectonic uplift of a forearc basin. Such short-lived platforms appear regularly in the geological record of the Costa Rican and Nicaraguan forearc basins. In Costa Rica, classical examples are the upper Campanian El Viejo and upper Paleocene-lower Eocene Barra Honda (Jaccard et al. 2001) Formations. The upper Oligocene–lower Miocene patch reef exposures of the Turrialba area of Costa Rica may be partly contemporaneous with the Juanilla Fm., but present far less extensive and less diverse coral communities.

References

Aguilar T (1999) Organismos de un arrecife fósil (Oligoceno Superior-Mioceno Inferior), del Caribe de Costa Rica. Rev Biol Trop 47:453–474

Aguilar T, Cortés J (2001) Arrecifes coralinos del Oligoceno Superior-Mioceno Inferior, de Turrialba, Costa Rica. Rev Biol Trop 49:203–213

Aigner T (1982) Event-stratification in nummulite accumulations and in shell beds from the Eocene of Egypt. In: Einsele G, Seilacher A (eds) Cyclic and event stratification. Springer, Berlin, pp 248–267

Aigner T (1985) Biofabrics as dynamic indicators in nummulite accumulations. J Sediment Petrol 55(1):131–134

Alvarado GE, Dengo C, Martens U, Bundschuh J, Aguilar T, Bonis SB (2007) Stratigraphy and geologic history. In: Bundschuh J, Alvarado GE (eds) Central America, geology, resources, hazards, vol 1. Taylor and Francis, pp 345–394

Amann H (1993) Randmarine und terrestrische Ablagerungsräume des neogenen Inselbogensystems in Costa Rica (Mittelamerika), vol 4. Profil, Stuttgart, p 161

Anthony KRN, Fabricius KE (2000) Shifting roles of heterotrophy and autotrophy in coral energetics under varying turbidity. J Exp Mar Biol Ecol 252:221–253

Arni P (1963) L'évolution des *Nummulitinae* en tant que facteur de modification des dépôts littoraux. In: Colloque International de Micropaléontologie, Dakar, Mai 1963, vol 32. Mém BRGM, pp 7–20

Astorga A (1987) El Cretácico Superior y el Paleógeno de la vertiente pacífica de Nicaragua meridional y Costa Rica septentrional:

Origen, evolución y dinámica de las cuencas profundas relacionadas al margen convergente de Centroamérica. Tesis de Licenciatura (unpublished), Universidad de Costa Rica, p 250

Astorga A (1988) Geodinámica de las cuencas del Cretácico Superior-Paleógeno de la región "forearc" del Sur de Nicaragua y Norte de Costa Rica. Rev Geol Am Central 9:1–40

Auer WF (1942) Summary report of paleontology of Pacific coast area, Nicaragua. p 18

Azéma J, Tournon J (1980) La péninsule de Santa Elena, Costa Rica: un massif ultrabasique charrié en marge pacifique de l'Amérique Centrale, Costa Rica. C R Acad Sci Paris 290:9–12

Azéma J, Tournon J (1982) The Guatemalan margin, the Nicoya Complex and the origin of the Caribbean plate. In: Aubouin J, von Huene R et al. (eds) Initial reports DSDP, vol 67. Washington (U.S. Govt. Printing Office), pp 739–745

Azéma J, Glaçon G, Tournon J (1981) Nouvelles données sur le Paléocène à Foraminifères planctoniques de la bordure pacifique du Costa Rica. C R Somm Soc Géol France 3:85–88

Baldermann A, Grathoff GH, Nickel C (2012) Micromilieu-controlled glauconitization in fecal pellets at Oker (central Germany). Clay Miner 47:513–538

Bally AW, Roberts DG, Sawyer D, Sinkewich A (2012) Cenozoic/Mesozoic and Paleozoic orogenic systems and their fold and thrust belts (FTBs). In: Roberts DG, Bally AW (eds) Regional geology and tectonics: Phanerozoic passive margins, cratonic basins and global tectonic maps, vol 1C. Elsevier, Amsterdam, pp 1042–1059

Bandini AN, Flores K, Baumgartner PO, Jackett SJ, Denyer P (2008) Late Cretaceous and Paleogene Radiolaria from the Nicoya Peninsula, Costa Rica: a tectonostratigraphic application. Stratigraphy 5:3–21

Bandini AN, Baumgartner PO, Flores K, Dumitrica P, Jackett SJ (2011) Early Jurassic to lower Late Cretaceous radiolarians from the Santa Rosa accretionary complex (northwestern Costa Rica). Ofioliti 36(1):1–35

Barboza G, Astorga A, Bottazzi G, Barrientos J, Muñoz A, Darce M, Duarte M, Espinoza M (1993) Integrated petroleum evaluation report, Pacific margin, Sandino Basin, Nicaragua. INE, internal report, pp 11–195

Baumgartner PO, Denyer P (2006) Evidence for middle Cretaceous accretion at Santa Elena Peninsula (Santa Rosa Accretionary Complex), Costa Rica. Geol Acta 4(1/2):179–191

Baumgartner PO, Mora CR, Butterlin J, Sigal J, Glacon G, Azéma J, Bourgois J (1984) Sedimentación y paleogeografía del Cretácico y Cenozoico del litoral pacífico de Costa Rica. Rev Geol Am Central 1:57–136

Baumgartner PO, Flores K, Bandini AN, Girault F, Cruz D (2008) Upper Triassic to Cretaceous radiolaria from Nicaragua and northern Costa Rica—the Mesquito composite oceanic terrane. Ofioliti 33:1–19

Baumgartner-Mora C, Denyer P (2002) Upper Cretaceous (Campanian-Maastrichtian) limestone with Larger Foraminifera from Peña Bruja Rock (Santa Elena Peninsula). Rev Geol Am Central 26:85–89

Baumgartner-Mora C, Baumgartner PO, Tschudin P (2008) Late Oligocene Larger Foraminifera from Nosara, Nicoya Península (Costa Rica) and Windward, Carriacou (Lesser Antilles), calibrated by 87Sr/86Sr isotope stratigraphy. Rev Geol Am Central 38:33–52

Behforouzi E, Safari A (2011) Biostratigraphy and Paleoecology of the Qom Formation in Chenar area (northwestern Kashan), Iran. Rev Mex Cienc Geol 28(3):555–565

Berhorst A (2006) Die Struktur des aktiven Kontinentalhangs vor Nicaragua und Costa Rica: marin-seismische Steil- und Weitwinkelmessungen. Ph.D. thesis, Christian Albrechts Universität, Kiel, p 153

Blow WH (1979) Danian to Oligocene planktonic foraminiferal biostratigraphy. In: Brill EJ (ed) The Cainozoic Globissinida. A study of the morphology, taxonomy, evolutionary relationships and the stratigraphical distribution of some Globigerinida (mainly Globigerinacea). EJB, Leiden, ix, pp 573–1413

Bosence DWJ (1991) Coralline algae: mineralization, taxonomy, and palaeoecology. In: Riding R (ed) Calcareous algae and stromatolites. Springer, Berlin, pp 98–113

Bosence DWJ (2005) A genetic classification of carbonate platforms based on their basinal and tectonic settings in the Cenozoic. Sediment Geol 175(1–4):49–72

Bosscher H, Schlager W (1992) Computer simulation of reef growth. Sedimentology 39:503–512

Bouma AH (1962) Sedimentology of some Flysch deposits: a graphic approach to facies interpretation. Elsevier, Amsterdam, p 168

Braga JC, Martín JM (1988) Neogene coralline-algal growth-forms and their palaeoenvironments in the Almanzora River Valley (Almeria, S.E. Spain). Palaeogeogr Palaeoclimatol Palaeoecol 67:285–303

Brasier MD (1995) Fossil indicators of nutrient levels. 2: evolution and extinction in relation to oligotrophy. In: Bosence DWJ, Allison PA (eds) Marine palaeoenvironmental analysis from fossils, vol 83. Geol Soc Am Spec Paper, pp 133–150

Briguglio A, Hohenegger J (2009) Nummulitids hydrodynamics: an example using *Nummulites globulus* Leymerie. Boll Soc Paleontol I 48(2):105–111

Briguglio A, Hohenegger J (2011) How to react to shallow-water hydrodynamics: the larger benthic foraminifera solution. Mar Micropaleontol 81:63–76

Buchs DM, Arculus RJ, Baumgartner PO, Baumgartner-Mora C, Ulianov A (2010) Late Cretaceous arc development on the SW margin of the Caribbean plate: insights from the Golfito, Costa Rica, and Azuero, Panama, complexes. Geochem Geophys Geosyst. doi:10.1029/2009GC002901

Budd AF (2000) Diversity and extinction in the Cenozoic history of Caribbean reefs. Coral Reefs 19(1):25–35

Butterlin J (1962) A propos de l'Oligocène dans la région des Caraïbes. Bull Soc Géol France 4(3):390–393

Butterlin J (1981) Claves para la determinacion de macroforaminiferos de Mexico y del Caribe, del Cretacico Superior al Mioceno Medio. Inst Mex Petr 29:1–51

Caudri CMB (1975) Geology and paleontology of Soldado Rock, Trinidad (West Indies). Eclogae Geol Helv 68:533–589

Caudri CMB (1996) The larger Foraminifera of Trinidad (West Indies). Eclogae Geol Helv 89:1137–1309

Chafetz HS, Reid A (2000) Syndepositional shallow-water precipitation of glauconitic minerals. Sediment Geol 136(1–2):29–42

Chapronière GCH (1975) Paleoecology of Oligo-Miocene larger foraminiferida, Australia. Alcheringa 1:37–58

Cheel RJ, Leckie DA (1993) Hummocky cross-stratification. In: Wright VP (ed) Sedimentology Review. Blackwell Scientific Publications, Oxford (UK), pp 103–122

Clerc C (1998) Foraminifères planctoniques en sections de la couverture du terrain de Nicoya (Costa Rica), Crétacé supérieur-Paléogène. Travail de diplôme, Université de Genève, p 121

Clifton HE (1988) Sedimentologic approaches to paleobathymetry, with applications to the Merced Formation of Central California. Palaios 3:507–522

Cole WS (1952) Eocene and Oligocene Larger Foraminifera from Panama Canal Zone and Vicinity, vol 244. US Geol Surv Prof Paper, p 41

Cole WS (1961) Some nomenclatural and stratigraphic problems involving Larger Foraminifera. Contrib Cushman Found Foram Res 12(4):136–147

Darce M, Duarte M (2002) Geologia de la Cuenca Sandino en costadentro, Nicaragua. Centro America, Instituto Nicaragüense de Energia, Managua, p 23

Dengo G (1962) Estudio Geológico de la Región de Guanacaste, Costa Rica. Instituto Geográfico Nacional, San José-Costa Rica, p 112

Dengo G (1985) Mid America: tectonic setting for the Pacific margin from southern Mexico to northwestern Columbia. In: Naim AEM, Stehli FG (eds) The Ocean basins and margins, vol 7. Plenum Press, New York, pp 123–180

Denyer P, Alvarado GE (2007) Mapa Geológico de Costa Rica 1: 400,000. Librería Francesa S.A

Di Marco G, Baumgartner PO, Chanell JET (1995) Late Cretaceous–early Tertiary paleomagnetic data and a revised tectonostratigraphic subdivision of Costa Rica and western Panama. In: Mann P (ed) Geologic and tectonic development of the Caribbean plate boundary in southern Central America, vol 295. Geol Soc Am Spec Paper, pp 1–27

Díaz de Gamero ML (1977) Estratigrafía y Micropalentología del Oligoceno y Mioceno Inferior del Centro de la Cuenca de Falcón, Venezuela, vol 22. Geos, Universidad Central de Venezuela, Caracas, pp 2–50

Dickinson WR (1995) Forearc basins. In: Busby CJ, Ingersoll RV (eds) Tectonics of Sedimentary Basins. Blackwell Science, pp 221–261

Dickinson WR, Seely DR (1979) Structure and stratigraphy of forearc regions. AAPG Bull 63:2–31

Dorobek SL (2008) Carbonate-platform facies in volcanic-arc settings: characteristics and controls on deposition and stratigraphic development. In: Draut AE, Clift PD, Scholl DW (eds) Formation and applications of the sedimentary record in Arc Collision Zones, vol 463. Geol Soc Am Spec Paper, pp 55–90

Dorr JB (1933) New data on the correlation of the Lower Oligocene of South and Central America with that of southern Mexico. J Paleontol 7(4):432–438

Dott RH, Bourgeois J (1982) Hummocky stratification: significance of its variable bedding sequences. Geol Soc Am Bull 93:663–680

Duke WL (1985) Hummocky cross-stratification, tropical hurricane, and intense winter storms. Sedimentology 32:167–194

Dullo WC (2005) Coral growth and reef growth: a brief review. Facies 51:33–48

Dumas S, Arnott RWC (2006) Origin of hummocky and swaley cross-stratification—the controlling influence of unidirectional current strength and aggradation rate. Geology 34(12):1073–1076. doi:10.1130/G22930A.1

Einsele G (2000) Sedimentary Basins. Evolution, facies, and sediment budget. Springer, Berlin Heidelberg GmbH, 2nd ed., p 792

Elming SA, Widenfalk L, Rodriguez D (eds) (1998) Investigación geocientifica en Nicaragua 1981–1991. Universidad Tecnologica de Lulea, Suecia, p 340

Escuder-Viruete J, Baumgartner PO (2014) Structural evolution and deformation kinematics of a subduction-related serpentinite-matrix mélange, Santa Elena Peninsula, northwest Costa Rica. J Struct Geol 66:356–381

Escuder-Viruete J, Baumgartner PO, Castillo-Carrión M (2015) Compositional diversity in ophiolitic peridotites as result of a multi-process history: the Santa Elena ophiolite, northwest Costa Rica. Lithos 231:16–34

Fagerstrom JA (1988) A structural model for reef communities. Palaios 3:217–220

Flores K (2009) Mesozoic Oceanic Terranes of Southern Central America—geology, geochemistry and geodynamics. Ph.D. thesis, Université de Lausanne, p 290

Flores K, Denyer P, Aguilar T (2003a) Nueva propuesta estratigráfica: geología de las hojas Matambú y Talolinga, Guanacaste, Costa Rica. Rev Geol Am Central 28:131–138

Flores K, Denyer P, Aguilar T (2003b) Nueva propuesta estratigráfica: Geología de la hoja Abangares, Guanacaste, Costa Rica. Rev Geol Am Central 29:127–136

Folk RL (1965) Some aspects of recrystallization in ancient limestones. In: Pray LC, Murray RS (eds) Dolomitization and Limestone Diagenesis, vol 13. SEPM Spec Publ, pp 14–48. doi:10.2110/pec.65.07.0014

Fravega P, Piazza M, Stockar R, Vannucci G (1994) Oligocene coral and algal reef and related facies of Valzemola (Savona, NW Italy). Riv It Paleont Strat 100(3):423–456

Frost SH, Langenheim RL (1974) Cenozoic reef biofacies. Northern Illinois University Press, DeKalb, p 388

Frost SH, Weiss MP (1979) Patch-reef communities and succession in the Oligocene of Antigua, West Indies. Geol Soc Am Bull 90:612–616

Frost SH, Harbour JL, Beach DK, Realini MJ, Harris PM (1983) Oligocene reef tract development, southwestern Puerto Rico, vol IX. Sedimenta, University of Miami, Rosenstiel School of Marine and Atmospheric Science, Miami, p 107

Funk J, Mann P, McIntosh K, Stephens J (2009) Cenozoic tectonics of the Nicaraguan depression, Nicaragua, and Median Trough, El Salvador, based on seismic-reflection profiling and remote-sensing data. Geol Soc Am Bull 121(11/12):1491–1521

Gazel E, Denyer P, Baumgartner PO (2006) Magmatic and geotectonic significance of Santa Elena Peninsula, Costa Rica. Geol Acta 4(1–2):193–202

Giunta G, Beccaluva L, Siena F (2006) Caribbean Plate margin evolution: constraints and current problems. Geol Acta 4(1–2):265–277

Hallock P, Glenn EC (1986) Larger Foraminifera: a tool for paleoenvironmental analysis of Cenozoic Carbonate depositional facies. Palaios 1(1):55–64

Hallock P, Schlager W (1986) Nutrient excess and the demise of coral reefs and carbonate platforms. Palaios 1(4):389–398

Haq BU, Al-Qahtani AM (2005) Phanerozoic cycles of sea-level change on the Arabian Platform. GeoArabia 10:127–160

Haq BU, Hardenbol J, Vail PR (1987) Chronology of fluctuating sea levels since the Triassic (250 million years ago to present). Science 235:1156–1167

Harrison JV (1953) The geology of the Santa Elena peninsula in Costa Rica, Central America. In: Proceedings of the Seventh Pacific Congress, vol 2. New Zealand, pp 102–104

Hauff F, Hoernle K, van den Bogaard P, Alvarado G, Garbe Schoenberg D (2000) Age and geochemistry of basaltic complexes in western Costa Rica; contributions to the geotectonic evolution of Central America. Geochem Geophys Geosyst 1:1009. doi:10.1029/1999GC000020

Hayes CW (1899) Physiography and geology of region adjacent to the Nicaragua canal route. Geol Soc Am Bull 10:285–448

Heckel PH (1974) Carbonate buildups in the geologic record: a review. In: Laporte LF (ed) Reefs in Time and Space, vol 18. SEPM Spec Publ, pp 90–154

Hedberg HD (ed) (1976) International Stratigraphic Guide: A Guide to Stratigraphic Classification, Terminology and Procedure. Wiley Interscience Publication, New York, 200 p

Hjulström F (1935) Studies of the morphological activity of rivers as illustrated by the River Fyris. Bull Geol Inst Univ Uppsala 25:221–527

Hodgson G (1998) Resumen de la geologia en el perfil geotransversal Nicaragüense—Estado del conocimiento 1984. In: Elming SA, Widenfalk L, Rodriguez D (eds) Investigación geocientifica en Nicaragua 1981–1991. Universidad Tecnologica de Lulea, Suecia, pp 41–51

Hoffstetter R, Dengo G, Dixon CG, Meyer-Abich H, Weyl R, Woodring WP, Zoppis Bracci L (1956) In: Hoffstetter R (ed) Lexique Stratigraphique International, vol V(2a). CNRS, Paris, pp 171–224

Hofmann HJ (1994) Grain-shape indices and isometric graphs. J Sediment Res 64(4a):916–920

Hottinger L (1997) Shallow benthic Foraminiferal assemblages as signals for depth of their deposition and their limitations. Bull Soc Géol France 168(4):491–505

Huggett JM, Gale AS (1997) Petrology and palaeoenvironmental significance of glaucony in the Eocene succession at Whitecliff Bay, Hampshire Basin, UK. J Geol Soc 154:897–912

Immenhauser A (2009) Estimating palaeo-water depth from the physical rock record. Earth-Sci Rev 96:107–139

Jaccard S, Münster M, Baumgartner PO, Baumgartner-Mora C, Denyer P (2001) Barra Honda (Upper Paleocene–Lower Eocene) and El Viejo (Campanian–Maastrichtian) carbonate platforms in the Tempisque area (Guanacaste, Costa Rica). Rev Geol Am Central 24:9–28

James NP (1983) Reef environment. In: Scholle PA, Bebout DG, Moore CH (eds) Carbonate depositional environments, vol 33. AAPG Memoir, pp 345–440

Johnson KG, Jackson JB, Budd AF (2008) Caribbean reef development was independent of coral diversity over 28 million years. Science 319(5869):1521–1523

Kelly JC, Webb JA (1999) The genesis of glaucony in the Oligo-Miocene Torquay Group, southeastern Australia: petrographic and geochemical evidence. Sediment Geol 125(1–2):99–114

Kennedy DM, Woodroffe CD (2002) Fringing reef growth and morphology: a review. Earth-Sci Rev 57:255–277

Kolb W, Schmidt H (1991) Depositional sequences associated with equilibrium coastlines in the Neogene of south-western Nicaragua. In: Macdonald DIM (ed) Sedimentation, tectonics and eustasy: sea-level changes at active margins, vol 12. SEPM Spec Publ, pp 259–272

Krawinkel H, Kolb W (1994) Sequential aspects of the El Fraile Formation (Nicaragua Through, SW Nicaragua). In: Seyfried H, Hellmann W (eds) Geology of an evolving Island arc: the isthmus of Southern Nicaragua, Costa Rica and Western Panamá, vol 7. Profil, Stuttgart, pp 325–333

Krawinkel H, Seyfried H, Calvo C, Astorga A (2000) Origin and inversion of sedimentary basins in southern Central America. Z Angew Geol SH 1:71–77

Kuang SJ (1971) Estudio geologico del Pacifico de Nicaragua. Division de Geologia, Catastro de Inventario de Recursos naturales 10:1–101

Kugler HG (2001) Paleocene to Holocene formations. In: Bolli HM, Knappertsbusch M (eds) Treatise on the Geology of Trinidad (part 4). Museum of Natural History, Basel, p 309

Lundberg N (1982) Evolution of the slope landward of the Middle America Trench, Nicoya Peninsula, Costa Rica. In: Leggett JK (ed) Trench-forearc geology, vol 10. Geol Soc London Spec Publ, pp 131–147

Matteucci R, Pignatti JS (1989) The taphonomy of *Nummulites*. Atti del Quarto Simposio di Ecologia e Paleoecologia delle Comunità Bentoniche, novembre 1988. Museo Regionale di Scienze Naturali, Torino, pp 183–198

McBirney A, Williams H (1965) Volcanic history of Nicaragua, vol 55. Univ Calif Publ Geol Sci, p 73

McIntosh KD, Silver EA, Ahmed I, Berhorst A, Ranero CR, Kelly RK, Flueh ER (2007) The Nicaragua convergent margin. In: Dixon TH, Moore JC (eds) The seismogenic zone of subduction thrust faults, Part III. Columbia University Press, New York, pp 257–287

Meschede M, Frisch W (1998) A plate tectonic model for the Mesozoic and Early Cenozoic history of the Caribbean plate. Tectonophysics 296:269–291

Miller KG, Kominz MA, Browning JV, Wright JD, Mountain GS, Katz ME, Sugarman PJ, Cramer BS, Christie-Blick N, Pekar SF (2005) The Phanerozoic record of global sea-level change. Science 310:1293–1298

Mitchell SF (2013) Stratigraphy of the White Limestone of Jamaica. Bull Soc Géol France 184(1–2):111–118

Molina E, Torres-Silva A, Coric S, Briguglio A (2016) Integrated biostratigraphy across the Eocene/Oligocene boundary at Noroña, Cuba, and the question of the extinction of orthophragminids. Newsl Stratigr 49(1):27–40

Monroe WH (1980) Geology of the Middle Tertiary formations of Puerto Rico, vol 953. US Geol Surv Prof Paper, p 93

Montaggioni LF (2005) History of Indo-Pacific coral reef systems since the last glaciation: development patterns and controlling factors. Earth-Sci Rev 71:1–75

Murphy MA, Salvador A (eds) (1999) International stratigraphic guide–an abridged edition. Episodes 22:255–271

Muscatine L, Porter JW (1977) Reef corals: mutualistic symbioses adapted to nutrient-poor environments. Bioscience 27(7):454–460

Mutti E, Tinterri R, Muzzi Magalhaes P, Basta G (2007) Deep-water turbidites and their equally important shallower-water cousins. AAPG Search and Discovery Article #50057, p 7

Myrow PM (1992) Bypass-zone tempestites facies and proximality trends for an ancient muddy shoreline and shelf. J Sediment Petrol 62(1):99–115

Parsons Corporation Report (1972) The geology of western Nicaragua. Nicaragua Tax Improvement and Natural Resources Inventory Project, Managua, p 220

Pearson PN, Olsson RK, Huber BT, Hemleben C, Berggren WA, Coxal HK (2006) Overview of Eocene planktonic foraminiferal taxonomy, paleoecology, phylogeny, and biostratigraphy. In: Pearson PN, Olsson RK, Huber BT, Hemleben C, Berggren WA (eds) Atlas of Eocene planktonic foraminifera, vol 41. Cushman Foundation Spec Publ, p 11–28

Ranero C, von Huene R, Flueh E, Duarte M, Baca D, McIntosh K (2000) A cross section of the convergent Pacific margin of Nicaragua. Tectonics 19(2):335–357

Ranero C, von Huene R, Weinrebe W, Barckhausen U (2007) Convergent margin tectonics: a marine perspective. In: Bundschuh J, Alvarado GE (eds) Central America, geology, resources, hazards, vol 1. Taylor and Francis, pp 239–265

Rasser MW, Riegl B (2002) Holocene coral reef rubble and its binding agents. Coral Reefs 21:57–72

RECOPE-INE (1993) Integrated Petroleum Evaluation Report, Pacific Margin, Sandino Basin, Nicaragua

Ricci Lucchi F (1995) Sedimentographica: a photographic atlas of sedimentary structures. Columbia University Press, New York, 2nd edn, p 255

Rivier F (1983) Síntesis geológica y mapa geológica del area del Bajo Tempisque, Guanacaste, Costa Rica. Inf Sem IGN 1:7–30

Robinson E, Wright RM (1993) Jamaican Paleogene larger foraminifera. In: Wright RM, Robinson E (eds) Biostratigraphy of Jamaica, vol 182. Geol Soc Am Memoir, pp 283–345

Rogers RD, Mann P, Emmet PA (2007) Tectonic terranes of the Chortis block based on integration of regional aeromagnetic and geologic data. In: Mann P (ed) Geologic and tectonic development of the Caribbean plate in northern Central America, vol 428. Geol Soc Am Spec Paper, pp 65–88. doi:10.1130/2007.2428(04)

Sallarès V, Meléndez A, Prada M, Ranero CR, McIntosh K, Grevemeyer I (2013) Overriding plate structure of the Nicaragua convergent margin: relationship to the seismogenic zone of the 1992 tsunami earthquake. Geochem Geophys Geosyst 14:3436–3461. doi:10.1002/ggge.20214

Saller AH, Reksalegora SW, Bassant P (2011) Sequence stratigraphy and growth of shelfal carbonates in a deltaic province, Kutai Basin, Offshore East Kalimantan, Indonesia. In: Morgan WA, George AD, Harris, PM, Kupecz JA, Sarg JF (eds) Cenozoic Carbonate Systems of Australasia, vol 96. SEPM Spec Publ, pp 147–174

Santra M, Steel RJ, Olariu C, Sweet ML (2013) Stages of sedimentary prism development on a convergent margin—Eocene Tyee

Forearc Basin, Coast Range, Oregon, USA. Global Planet Change 103:207–231

Sartorio D, Venturini S (1988) Southern Tethys biofacies. San Donato Milanese (Agip), p 235

Saunders JB, Jung P, Biju-Duval B (1986) Neogene Paleontology in the Northern Dominican Republic: 1. Field surveys, lithology, environment, and age. Bull Am Paleontol 89(323):1–79

Schmidt-Effing R (1974) El primer hallazgo de amonites en América Central Meridional y notas sobre facies cretácicas en dicha región. Inf Sem IGN 1:53–61

Schmidt-Effing R (1979) Alter und Genese des Nicoya-Komplexes, einer ozeanischen Paläokruste (Oberjura bis Eozän) im südlichen Zentralamerika. Geol Rundsch 68:457–494

Schmidt-Effing R (1980) Radiolarien der Mittel-Kreide aus dem Santa Elena-Massiv von Costa Rica. Neues Jahrb Geol Paläontol 160(2):241–257

Schuster F, Wielandt U (1999) Oligocene and Early Miocene coral faunas from Iran: palaeoecology and palaeobiogeography. Int J Earth Sci 88:571–581

Seddighi M, Briguglio A, Hohenegger H, Papazzoni CA (2015) New results on the hydrodynamic behaviour of fossil *Nummulites* tests from two nummulite banks from the Bartonian and Priabonian of northern Italy. Boll Soc Paleontol I 54(2):103–116

Seyfried H, Sprechmann P (1985) Acerca de la formación del puente-istmo Centroamericano Meridional, con énfasis en el desarrollo acaecido desde Campanénse al Eoceno. Rev Geol Am Central 2:63–87

Seyfried H, Astorga A, Ammann H, Calvo C, Kolb W, Schmidt H, Winsemann J (1991) Anatomy of an evolving island arc: tectonic and eustatic control in the south Central American forearc area. In: Macdonald DIM (ed) Sedimentation, Tectonics and Eustasy: Sea-Level Changes at Active Margins, vol 12. SEPM Spec Publ, pp 217–240

Seyrafian A, Vasiri-Moghaddam H, Arzeni N, Taheri A (2011) Facies analysis of the Asmari Formation in central and north-central Zagros basin, southwest Iran: biostratigraphy, paleoecology and diagenesis. Rev Mex Cienc Geol 28(3):439–458

Sprechmann P, Astorga A, Calvo C, Fernández A (1994) Stratigraphic chart of the sedimentary basins of Costa Rica, Central America. In: Seyfried H, Hellmann W (eds) Geology of an evolving Island arc: The isthmus of Southern Nicaragua, Costa Rica and Western Panamá, vol 7. Profil, Stuttgart, pp 427–433

Stemann TA (2004) Reef corals of the White Limestone Group of Jamaica. Cainozoic Res 3(1–2):83–107

Struss I, Brandes C, Blisniuk PM, Winsemann J (2007) Eocene deep-water channel-levee deposits, Nicaragua: Channel geometries and internal deformation patterns of six outcrops. In: Nilsen TH, Shew RD, Steffens GS, Studlick JRJ (ed) Atlas of deep-water outcrops, vol 56. AAPG Studies in Geology, CD-ROM, p 31

Struss I, Artiles V, Cramer B, Winsemann J (2008) The petroleum system in the Sandino forearc basin, offshore western Nicaragua. J Pet Geol 31:221–244. doi:10.1111/j.1747-5457.2008.00418.x

Tournon J (1984) Magmatismes du Mésozoique à l'actuel en Amérique Centrale: l'exemple du Costa Rica, des ophiolites aux andésites. Ph.D. thesis, University Pierre and Marie Curie, Paris, p 335

Tournon J (1994) The Santa Elena Peninsula: an ophiolitic nappe and a sedimentary volcanic relative autochthonous. In: Seyfried H, Hellmann W (eds) Geology of an evolving Island arc: the isthmus of Southern Nicaragua, Costa Rica and Western Panamá, vol 7. Profil, Stuttgart, pp 87–96

Tucker ME (1993) Carbonate diagenesis and sequence stratigraphy. In: Wright VP (ed) Sedimentology review. Blackwell, Oxford, pp 51–72

Vaughan TW (1918) Geological history of Central America and the West Indies during Cenozoic time. Geol Soc Am Bull 29:615–630

Vaughan TW (1919) Fossil corals from Central America, Cuba, and Porto Rico with an account of the American Tertiary, Pleistocene, and recent coral reefs. USA Natl Mus Bull 103:189–524

Vaughan TW, Cooke W, Condit DD, Ross CP, Woodring WP, Alkins FC (1921) Geological survey of the Dominican Republic, vol 1. USGS, Gibson Brothers Press, Washington D.C., p 268

Walker RG, Duke WL, Leckie DA (1983) Hummocky stratification: significance of its variable bedding sequences: discussion. Geol Soc Am Bull 94:1245–1249

Walther CHE, Flueh ER, Ranero CR, Von Huene R, Strauch W (2000) Crustal structure across the Pacific margin of Nicaragua: evidence for ophiolitic basement and a shallow mantle sliver. Geophys J Int 141:759–777

Weinberg RF (1992) Neotectonic development of western Nicaragua. Tectonics 11(5):1010–1017

Weiss MP (1994) Oligocene limestones of Antigua, West Indies: Neptune succeeds Vulcan. Caribb J Sci 30:1–29

Weyl R (1980) Geology of Central America. Gebruder Borntraeger, Berlin, p 371

Williams RL (1972) The geology of western Nicaragua. Catastro-Managua

Wilson TC (1942) Geology of Pacific Coast area, Nicaragua, summary report. Geological Survey of Nicaragua, Managua

Wilson MEJ (2005) Equatorial delta-front patch reef development during the Neogene, Borneo. J Sediment Res 75(1):116–134

Wilson MEJ, Hall R (2010) Tectonic influences on SE Asian carbonates and their reservoir development. In: Morgan WA, George AD, Harris PM, Kupecz JA, Sarg JF (eds) Cenozoic carbonate systems of Australasia, vol 95. SEPM Spec Publ, pp 13–40

Wilson MEJ, Lokier SJ (2002) Siliciclastic and volcaniclastic influences on equatorial carbonates; insights from the Neogene of Indonesia. Sedimentology 49(3):583–601

Winsemann J (1992) Tiefwasser-Sedimentationsprozesse und -produkte in den Forearc-Becken des mittelamerikanischen Inselbogensystems: Eine sequenzstratigraphische Analyse, vol 2. Profil, Stuttgart, p 218

Winsemann J, Seyfried H (1991) Response of deep-water fore-arc systems to sea-level changes, tectonic activity and volcaniclastic input in Central America. In: Macdonald DIM (ed) Sedimentation, tectonics and eustasy: sea-level changes at active margins, vol 12. SEPM Spec Publ, pp 273–292

Wood R (1999) Reef evolution. Oxford University Press, Oxford, p 414

Wood R (2011) General evolution of carbonate reefs. In: Hopley D (ed) Encyclopedia of modern coral reefs: structure, form and process. Springer, Amsterdam, pp 452–469

Zaccarini F, Garuti G, Proenza JA, Campos L, Thalhammer OAR, Aiglsperger T, Lewis JF (2011) Chromite and platinum group elements mineralization in the Santa Elena Ultramafic Nappe (Costa Rica): geodynamic implications. Geol Acta 9(3/4):407–423

Zoppis Bracci L, Del Giudice D (1958) Geologia de la costa del Pacifico de Nicaragua. Bol Serv Geol Nac Nicaragua 2:19–68